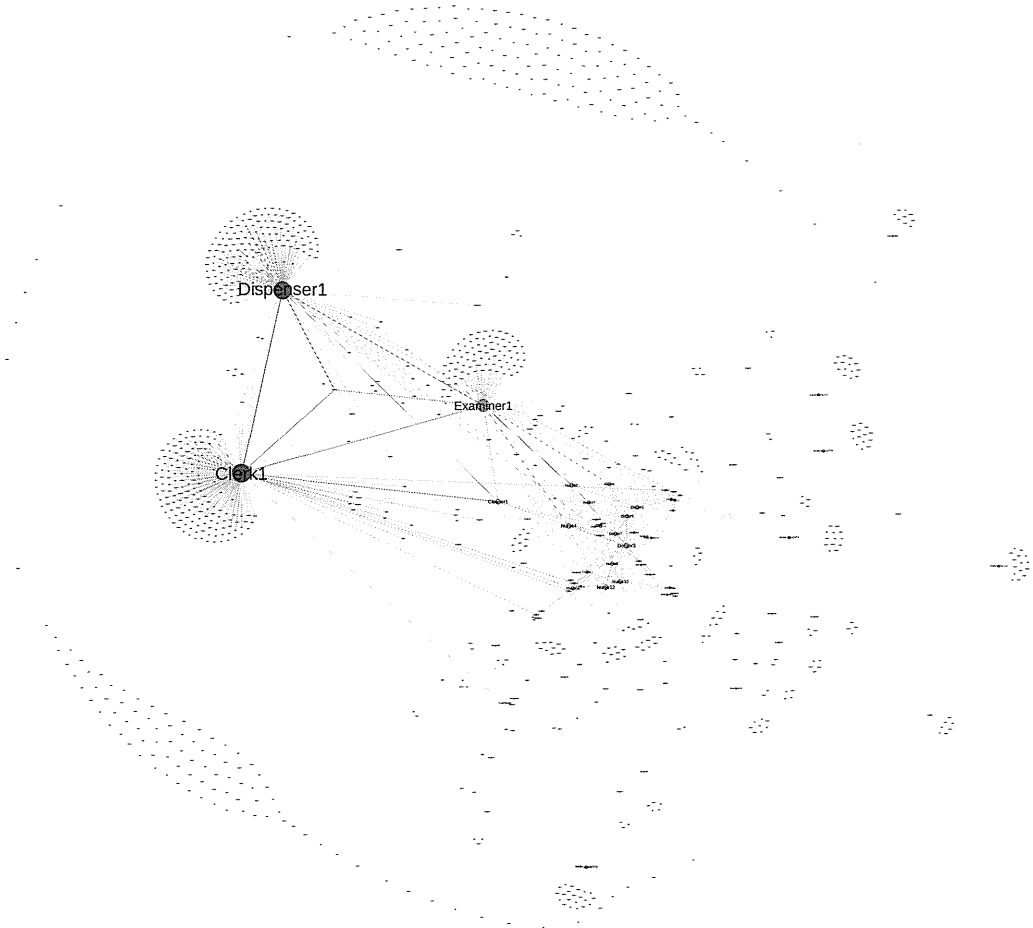

Fig. 8 Visualization of contact network in scenario D

- Nodes that represent nurses, doctors and inpatients are attracted into the center of the graph (Figure 9). It implies that frequent close contacts were made between them.

Figure 9 shows the center of the risk graph, in which close contacts between doctors, nurses and inpatients are illustrated. The nodes which are marked by blue explosion shapes represent health care workers who have been infected during the simulation. We can see that those agents are at the center of the risk graph and are have frequent contacts with inpatients. The nodes which represent doctors and nurses who has been infected during the simulation arose on top of the list of node in descending order of degree. However, the dispenser and the clerk were not infected, even though nodes represent them have a high degree. It can be explained that most of the contacts they made were with outpatients, so their risk of infection were low. The risk can also be evaluated by Spot Contamination Level of the place that the two staff were working in Figure 6. The Figure shows that staff area and operation area where the two staff work are less contaminated than ward area. It means that infection risk of those staff is lower than risk infection of nurses who almost working with inpatient in ward area.

Several conclusions can be drawn from analysis on risk graph are:

- Two nodes are spatially closer if they have a close and frequent contact.
- Close and frequent contacts between agents will attract them into center of the graph.
- Risk of infection can be assessed not only by the degree of the nodes but also by the amount of close contacts.

The visualization of risk graph demonstrated above can be a valid method to assess infection risk but it is not completed. The nature of contact that transmit virus cannot be seen from the graph. However, thanks to the development of large networks graphs visualization software, such as Gephi, we can highlight and track all contacts of agents in real time. An integration with

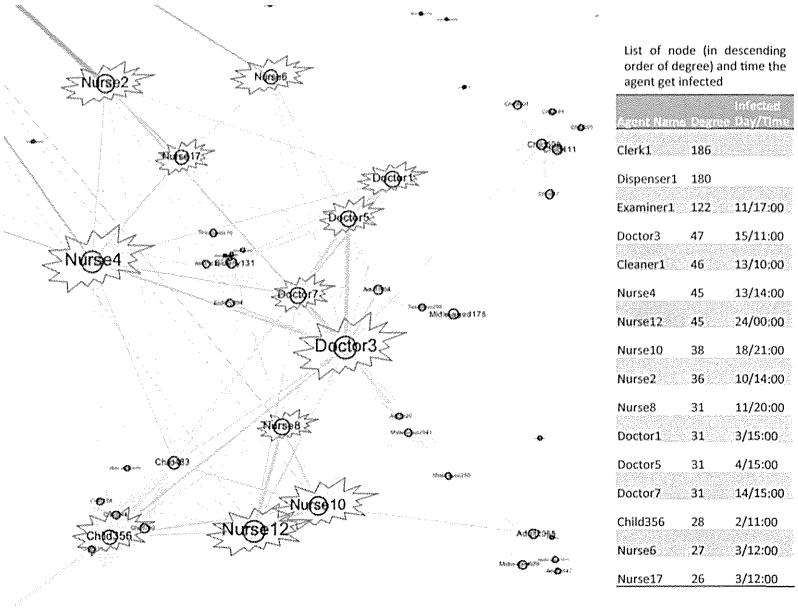

List of node (in descending order of degree) and time the agent get infected

Agent Name	Degree	Infected Day/Time
Clerk1	186	
Dispenser1	180	
Examiner1	122	11/17:00
Doctor3	47	15/11:00
Cleaner1	46	13/10:00
Nurse4	45	13/14:00
Nurse12	45	24/00:00
Nurse10	38	18/21:00
Nurse2	36	10/14:00
Nurse8	31	11/20:00
Doctor1	31	3/15:00
Doctor5	31	4/15:00
Doctor7	31	14/15:00
Child356	28	2/11:00
Nurse6	27	3/12:00
Nurse17	26	3/12:00

Fig. 9 Center of the risk graph and list of infected health care workers in scenario D

human real time tracking systems can be potential for tracking and detecting ”dangerous” contacts between health care workers or between health care workers and patients.

VI.CONCLUSION AND DISCCUSSION

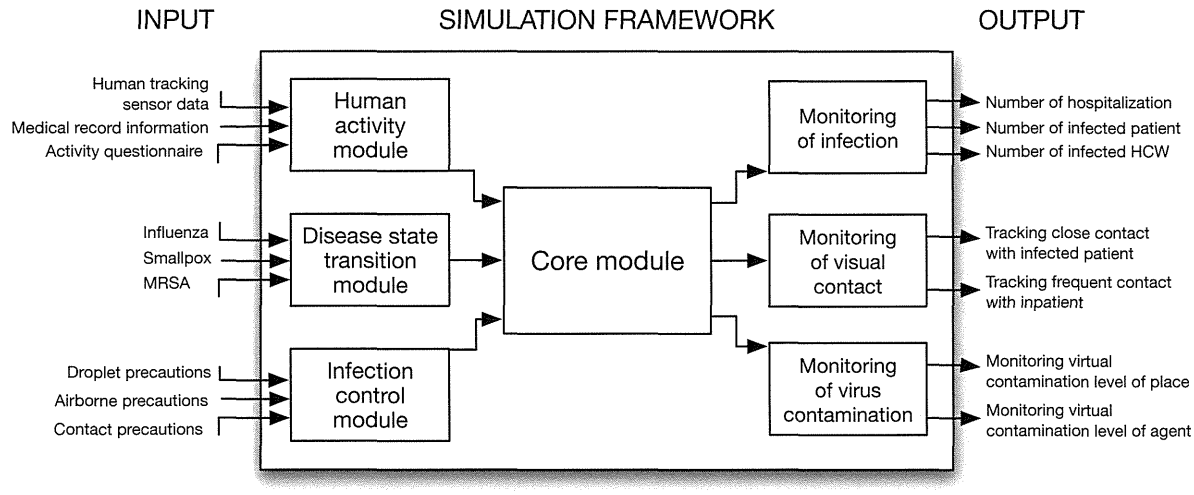

Fig. 10 Structure of the simulation framework.

We have built a simulation model for infection of an influenza-like illness in an artificial hospital and quantitatively assessed infection risk of the diseases. The simulation results have shed more light on epidemiological belief of that direct patient care HCW have high risk of catching nosocomial influenza virus and that staff washing hand and wearing mask are effective to prevent an outbreak of the disease in the hospital. The methodology of quantification and visualization the infection risk have been demonstrated and they are innovative contributions to literature which has been dominated by experience. The original approach has provided us a potential methodology for risk management in infection control of nosocomial infection.

Although data and knowledge for the model have been been constructed based on two field works onsite, due to the lack of statistics data and impossibility of taking those experiments in a hospital, empirical validation of the model could not be conducted. To introduce data of human activity within a real hospital to validate the model is our further work.

Although still under development, the future work is to integrate real data collecting by sensor to the simulation framework. The structure of the simulation framework is illustrated in Figure 10. We have developed and used wireless tracking systems to track real-time movement of humans in a building. The real data of movement of patients and health care workers in a real hospital can be achieved. Activity pattern of people can also be collected via activity questionnaire. Changing parameters of the disease transition module can be applied to study other infectious diseases. Infection control measures can be changed in many scenarios depending on infection control resources of the hospital. The core module inherits from the current module but can be rebuilt to fit the structure of a new hospital. Simulation output shows real-time graph of the number of hospitalization, infected patient and HCW. By visualizing contact network, close and frequent contact with high risk patients can be tracked and monitored. Variation of virtual virus contamination level of places and agents can be monitored in real time. The simulation framework could be a potential decision-making support tool for hospital administrators to evaluate nosocomial infection control and it can also be used as an educational tool to study nosocomial infection.

REFERENCES

[1] KKlevens, R. Monina, et al. "Estimating health care-associated infections and deaths in US hospitals, 2002." Public health reports vol. 122.2, pp. 160-166, 2007.

[2] H.C.Maltezoua, M. Drancourt. "Nosocomial influenza in children." Journal of Hospital Infection. vol. 55, pp. 83-91, 2003.

[3] Bridges, Carolyn B., et al. "Prevention and control of influenza. Recommendations of the Advisory Committee on Immunization Practices (ACIP)." MMWR. Recommendations and reports: Morbidity and mortality weekly report. Recommendations and reports/Centers for Disease Control 51.RR-3, pp. 1-31, 2002.

[4] Sebille, V. & Valleron. A. J. "A computer simulation model for the spread of nosocomial infections caused by multidrug-resistant pathogens." Computers and Biomedical Research vol. 30(4), pp. 307322, 1997.

[5] Triola, M.M., Holzman, R.S. "Agent-based simulation of nosocomial transmission in the medical intensive care unit." Computer-Based Medical Systems, 2003. Proceedings. 16th IEEE Symposium. IEEE, pp. 284-288, 2003.

[6] Boon Som Ong, Mark Chen, Vernon Lee, Joc Cing Tay. "An Individual-Based Model of Influenza in Nosocomial Environments." Lecture Notes in Computer Science. vol. 5101/2008, pp. 590-599, 2008.

[7] Meng, Yang, et al. "An application of agent-based simulation to the management of hospital-acquired infection." Journal of Simulation vol. 4.1, pp. 60-67, 2010.

[8] Laskowski, Marek, et al. "Agent-based modeling of the spread of influenza-like illness in an emergency department: a simulation study." Information Technology in Biomedicine, IEEE Transactions on vol. 15(6), pp. 877-889, 2011.

[9] N. Gilbert. "Agent-based model: Quantitative applications in the social sciences." SAGE Publications, pp. 38-46, 1999.

[10] N. Gilbert, K.Troitzsch. "Simulation for the Social Scientist." Open University Press, pp. 199-215, 2005.

[11] El-Sayed, Abdulrahman M., et al. "Social network analysis and agent-based modeling in social epidemiology." Epidemiologic Perspectives & Innovations 9.1, 2002.

[12] Longini, Ira M., et al. "Containing pandemic influenza at the source." Science vol. 309.5737, pp. 1083-1087, 2005.

[13] M.J. Keeling, M.E. Woolhouse et al. "Modelling vaccination strategies against foot-and-mouth disease." Nature vol.421, pp. 136142, 2003.

[14] Meyers, Lauren Ancel, et al. "Applying network theory to epidemics: control measures for Mycoplasma pneumoniae outbreaks." Emerging infectious diseases vol. 9.2, pp. 204-210, 2003.

[15] Ichikawa, M., Koyama, Y., Deguchi, H. "Virtual City Model for Simulating Social Phenomena." Agent-Based Social Systems vol. 7, pp. 253-264, 2010.

[16] Tanuma, H., Deguchi, H., Shimizu, T. "SOARS: Spot Oriented Agent Role Simulator - Design and Implementation." Agent-Based Simulation: From Modeling Methodologies to Real-World Applications, pp. 1-15, 2005.

[17] Bean, B., et al. "Survival of influenza viruses on environmental surfaces." Journal of infectious diseases vol. 146.1, pp. 47-51, 1982.

[18] Centers for Disease Control and Prevention. "Prevention Strategies for Seasonal Influenza in Healthcare Settings". http://www.cdc.gov/flu/professionals/infectioncontrol/healthcaresettings.htm. Accessed January 25, 2011.

[19] Munster, Vincent J., et al. "Pathogenesis and transmission of swine-origin 2009 A (H1N1) influenza virus in ferrets." Science vol. 325.5939, pp. 481-483, 2009.

[20] Naffakh, Nadia, and Sylvie Van Der Werf. "April 2009: an outbreak of swine-origin influenza A (H1N1) virus with evidence for human-to-human transmission." Microbes and infection vol. 11.8, pp. 725-728, 2009.

[21] Malik Peiris, J. S., Leo LM Poon, and Yi Guan. "Emergence of a novel swine-origin influenza A virus (S-OIV) H1N1 virus in humans." Journal of Clinical Virology vol. 45.3, pp. 169-173, 2009.

[22] Choi, Young Ki, et al. "Studies of H5N1 influenza virus infection of pigs by using viruses isolated in Vietnam and Thailand in 2004." Journal of virology vol. 79.16, pp. 10821-10825, 2005.

[23] H. Deguchi, T. Saito, M. Ichikawa, H. Tanuma. "Simulated Tabletop Exercise for Risk Management - Anti Bio-Terrorism Multi Scenario Simulated Tabletop Exercise." Development in Business Simulation and Experimental Learning, vol.38, p.1-21, 2011.

[24] Glasser, John, et al. "Evaluation of targeted influenza vaccination strategies via population modeling." PloS one 5.9: e12777, 2010.

[25] Grayson, M. Lindsay, et al. "Efficacy of soap and water and alcohol-based hand-rub preparations against live H1N1 influenza virus on the hands of human volunteers." Clinical Infectious Diseases vol. 48.3, pp. 285-291, 2009.

[26] Loeb, Mark, et al. "Surgical mask vs N95 respirator for preventing influenza among health care workers: a randomized trial." Jama vol. 302.17, pp. 1865-1871, 2009.

[27] Otter, J. A., et al. "Assessing the biological efficacy and rate of recontamination following hydrogen peroxide vapour decontamination." Journal of Hospital Infection vol. 67.2, pp. 182-188, 2007.

[28] Cowling, Benjamin J., et al. "Facemasks and Hand Hygiene to Prevent Influenza Transmission in HouseholdsA Cluster Randomized Trial." Annals of Internal Medicine vol. 151.7, pp. 437-446, 2009.

[29] Aiello, Allison E., et al. "Facemasks, hand hygiene, and influenza among young adults: a randomized intervention trial." PloS one 7.1: e29744, 2012.

[30] Bastian, M., Heymann, S., Jacomy, M. "Gephi: an open source software for exploring and manipulating networks." ICWSM pp. 361-362, 2009.

Trans R Soc Trop Med Hyg 2014; **108**: 768–773
doi:10.1093/trstmh/tru163 Advance Access publication 24 October 2014

ORIGINAL ARTICLE

Development and validation of serological assays for viral hemorrhagic fevers and determination of the prevalence of Rift Valley fever in Borno State, Nigeria

David Nadeba Bukbuk[a], Shuetsu Fukushi[b,*], Hideki Tani[b], Tomoki Yoshikawa[b], Satoshi Taniguchi[b], Koichiro Iha[b], Aiko Fukuma[b], Masayuki Shimojima[b], Shigeru Morikawa[c], Masayuki Saijo[b], Francis Kasolo[d] and Saka Saheed Baba[a]

[a]Department of Microbiology and Parasitology, Faculty of Veterinary Medicine, University of Maiduguri, Maiduguri, Nigeria; [b]Department of Virology 1, National Institute of Infectious Diseases, Tokyo, Japan; [c]Department of Veterinary Science, National Institute of Infectious Diseases, Tokyo, Japan; [d]Disease Prevention and Control Cluster at the WHO Regional Office for Africa, Congo-Brazzaville

*Corresponding author: Tel: +81425610771; E-mail: fukushi@nih.go.jp

Received 10 April 2014; revised 10 September 2014; accepted 11 September 2014

Background: Rift Valley fever (RVF) is endemic to the tropical regions of eastern and southern Africa. The seroprevalence of RVF was investigated among the human population in Borno State, Nigeria to determine the occurrence of the disease in the study area in comparison with that of Lassa fever and Crimean-Congo Hemorrhagic fever.

Methods: Recombinant nucleoprotein (rNP)-based IgG-ELISAs for the detection of serum antibodies against RVF virus (RVFV), Lassa fever virus (LASV), and Crimean-Congo hemorrhagic fever virus (CCHFV) were used to test human sera in Borno State, Nigeria. The presence of neutralizing antibody against the RVFV-glycoprotein-bearing vesicular stomatitis virus pseudotype (RVFVpv) was also determined in the human sera.

Results: Of the 297 serum samples tested, 42 (14.1%) were positive for the presence of RVFV-IgG and 22 (7.4%) and 7 (2.4%) of the serum samples were positive for antibodies against LASV and CCHFV, respectively. There was a positive correlation between the titers of neutralizing antibodies obtained using RVFVpv and those obtained using the conventional neutralization assay with the attenuated RVFV-MP12 strain.

Conclusions: The seroprevalence of RVF was significantly higher than that of LASV and CCHF in Borno State, Nigeria. The RVFVpv-based neutralization assay developed in this study has the potential to replace the traditional assays based on live viruses for the diagnosis and seroepidemiological studies of RVF.

Keywords: Nigeria, Rift Valley fever, Seroprevalence

Introduction

Rift Valley fever virus (RVFV) is a zoonotic mosquito-borne virus belonging to the genus *Phlebovirus* in the Family *Bunyaviridae*. It causes severe diseases in humans and livestock throughout Africa[1] and the Arabian Peninsula[2]. RVFV is also considered to be a potential bioterrorism agent. In the last few decades, Rift Valley fever (RVF) outbreaks have been reported in eastern and southern Africa (e.g. Kenya, Somalia, United Republic of Tanzania, Madagascar and South Africa).[3–7] In contrast, there have been very few reports on the recent occurrence of RVF in western and central Africa. Significant high- and low-prevalence clusters of RVF in sub-national areas on the African continent have been reported.[8] Since the spread of RVFV largely depends on the mosquito vectors and the translocation of animal hosts, an endemic situation usually occurs in the restricted geographical areas inhabited by their hosts and vectors. In Nigeria, RVFV antibodies have been found in sheep, goats, cattle, horses and camels in the northern states of Kaduna and Sokoto[9] and in the plateau area[10] suggesting that the virus may be enzootic in Nigeria. In addition, serological studies conducted on human sera have confirmed the existence of the disease in Nigeria.[11] The specific geographical location of Borno State in northeastern Nigeria, which shares international borders with three other African countries (Cameroun, Chad and Niger), makes it vulnerable to the transboundary spread of various diseases, including viral hemorrhagic fevers (VHFs). In addition, Borno State has been reported as the niche for Lassa fever virus (LASV) and possibly other VHFs. However, the epidemiology of RVF and other VHFs has not been extensively investigated in Borno State. A detailed and accurate investigation of the seroprevalence is necessary to ascertain the occurrence and spread of RVF in this area.

RVFV possesses a single-stranded tripartite RNA genome composed of three segments: S, M and L. The S segment encodes the nucleocapsid protein (NP) and non-structural (NS) protein, using an ambisense strategy. The M segment encodes the precursor for the glycoproteins Gn and Gc and two non-structural proteins of 78 kDa and 14 kDa. The L segment encodes the L protein.[12] The nucleotide sequence of the NP gene is highly conserved among various RVFV strains.[13] Serum antibodies against NP are readily detected early after infection and in convalescent individuals, providing a basis for the diagnosis of RVF.[14,15]

The traditional diagnostic assays for VHFs are based on immunoassays that use live viruses as the source of capture antigens. The use of highly attenuated RVFV (RVFV-MP12) does not require stringent biosafety measures and could readily be adopted in laboratories in developing countries where infrastructures for biosafety level 3 or 4 containments are lacking. The usefulness of recombinant viral nucleoprotein (rNP)-based serological assays, such as IgG-ELISAs and immunofluoresence assays (IFAs) for the detection of antibodies against VHFs such as Crimean-Congo hemorrhagic fever virus (CCHFV) and LASV have been reported.[16–18] Recombinant protein technology does not require high containment biosafety facilities and could readily meet the demand for a simple and reliable system not only for diagnosis of VHFs but also for comparative seroepidemiology of various VHFs in a cohort study.

In this study, the seroprevalence of RVFV infection in humans in Borno State, Nigeria, was determined using rNP-based IgG ELISAs, and the prevalence of RVFV antibody was compared with those of other hemorrhagic fever virus infections including LASV and CCHFV. In addition, we developed virus neutralization assays using vesicular stomatitis virus (VSV) pseudotype virus-bearing glycoproteins of RVFV, and the usefulness of the VSV pseudotype system was determined for a high throughput screening of neutralizing antibodies against RVFV.

Materials and methods

Serum samples

Two hundred and ninety-seven serum samples were collected between September 2011 and February 2012 from patients attending health facilities (government hospitals, private hospitals or clinics) in 10 out of the 27 local government areas (LGAs) in Borno State in northern Nigeria. A simple random sampling technique was used to obtain human sera from the selected LGAs, which consisted of at least three LGAs from each of the three senatorial districts (North, Central and South), and also from the town of Lassa.

Expression and purification of rNPs

Insect Tn5 cells[19] were infected with recombinant baculoviruses expressing rNPs of RVFV, LASV or CCHFV to produce recombinant His-tagged RVFV-rNP, LASV-rNP or CCHFV-rNP, respectively.[16,17,19] The rNPs were purified by Ni^{2+} column chromatography (QIAGEN GmbH, Hilden, Germany), as described previously.[17] The negative control antigen (ΔP) was prepared from a baculovirus (Ac-ΔP) that lacks polyhedrin expression using the same protocols as for the rNPs. Expression of the His-tagged rNPs and ΔP was analyzed by SDS-PAGE gels (12% polyacrylamide) stained with Coomassie blue (Bio-Rad Laboratories, Hercules, CA, USA) (Supplementary Figure 1).

IgG-ELISA

IgG-ELISA was performed as described previously.[16] Briefly, 96-well ELISA plates were coated with the predetermined optimal quantity of purified RVFV-rNP, LASV-rNP or CCHFV-rNP (approximately 100 ng/well) at 4°C overnight. Each well of the plates was then covered with 200 μl of PBS containing 5% skim milk and 0.05% Tween 20 (Sigma, St. Louis, MO, USA) (PBST-M), followed by incubation for 1 h at 37°C for blocking. The plates were washed three times with PBS containing 0.05% Tween 20 (PBST) and then inoculated with test serum (100 μl/well), which was diluted 1:400 and 1:1600 with PBST-M. After a 1 h incubation period, the plates were washed three times with PBST and then were inoculated with goat anti-human IgG antibody labeled with HRP (1:1000 dilution; Zymed Laboratories, Inc., South San Francisco, CA, USA). After a further 1 h incubation period, the plates were washed and 100 μl of ABTS solution (Roche Diagnostics, Mannheim, Germany) was added to each well. The plates were incubated for 30 min at room temperature, and the optical density at 405 nm (OD_{405}) was measured against a reference of 490 nm. The adjusted OD_{405} value was calculated by subtracting the OD_{405} value of the negative Ag-coated wells from that of the corresponding wells. The mean plus three standard deviations (mean+3SD) of the ELISA indices for the IgG-ELISAs was calculated using human serum samples that were confirmed to be negative for infection with the respective viruses by IFA (data not shown) and was used as the cut-off value for the IgG-ELISAs. In order to minimize false-positive results that could occur with single serum dilution, IgG response was considered to be positive if the sample showed adjusted OD_{405} values above the cut-off at both 1:400 and 1:1600 dilutions.

Conventional neutralization assay

The conventional neutralization assay using infectious RVFV (RVFV-MP12 strain) was performed as described previously.[20] Briefly, heat-inactivated serum samples were diluted three-fold (from 1:40 to 1:1080) with Eagle's minimum essential medium (MEM, Sigma, St. Louis, MO, USA) containing 2% FBS (Invitrogen, Carlsbad, CA, USA). Each test sample (50 μl) was then mixed with the same volume of RVFV-MP12 at an infectious dose of 100 plaque forming units. The mixture was then incubated for 1 h at 37°C for neutralization. After incubation, the mixtures were tested for neutralization by the cytopathic effect inhibition assay using Vero E6 cells.[20] The neutralization antibody (NAb) titer was defined as the reciprocal of the highest dilution at which no cytopathic effect was observed.

Generation of VSV pseudotyped with RVFV-glycoprotein

The glycoprotein (GP) cDNA of RVFV-MP12 was cloned into the pKS336 vector[17] to construct an RVFV-GP expression plasmid, designated as pKS336-RVFV-GP. To generate the RVFV-GP-bearing VSV pseudotype (RVFVpv), a *G-VSVΔG/luc encoding luciferase gene (kindly provided by Dr. M. A. Whitt), instead of the VSVG gene, was inoculated into human kidney 293 T cells[21] transfected

with pKS336-RVFV-GP. After 24 h the culture supernatants were collected and used as a working seed for the RVFVpv.

Neutralization test using RVFVpv

The dilution of RVFVpv used was calculated to produce approximately 10^5 relative light units in control wells. Serum samples were mixed with RVFVpv at a dilution of 1:50 in MEM (Sigma) supplemented with 2% FBS (Invitrogen). Then, the mixture was incubated at 37°C for 1 h for neutralization. The serum-RVFVpv mixture was transferred to 96-well plates containing monolayers of Vero E6 cells.[20] After 24 h the cells were lysed, and the luciferase activities were measured using the Bright-Glo Luciferase Assay System (Promega, Madison, WI, USA) according to the protocol recommended by the manufacturer.

Statistical methods

The sensitivity, specificity and predictive values for positive and negative tests were calculated by standard methods. Spearman's rank correlation coefficient test, ROC curves and two-graph-ROC (TG-ROC) curves[22,23] were analyzed using the Stat Flex ver. 5 software program (Artech Co. Ltd., Osaka, Japan).

Results

rNP-based IgG-ELISA

In order to determine the seroprevalence of RVFV in humans in Borno State, Nigeria, sera were first subjected to an His-RVFV-rNP-based IgG-ELISA. An IgG response was considered to be positive if the sample had adjusted OD_{405} values higher than cut-off values at both 1:400 and 1:1600 dilutions. Of the 297 serum samples analyzed, 42 (14.1%) were positive for RVFV IgG (Table 1). Simultaneously, the serum samples were also tested for the presence of antibodies against LASV and CCHFV using the rNP-based IgG ELISAs, and a total of 22 (7.4%) and 7 (2.4%) of the samples were positive for antibodies against LASV and CCHFV, respectively (Table 1). The result indicated a high prevalence rate of RVF in the study area.

In order to confirm the efficacy of RVFV-rNP as an antigen and to determine the sensitivity and specificity of the RVFV-rNP based ELISA, the NAb assay was performed using RVFV-MP12. Of the 271 human serum samples examined, 34 (12.6%) were positive for NAb, with antibody titers ranging from 40 to 1080 (Table 1). Thirty-one out of 34 (sensitivity: 91.2%) NAb-positive samples were also positive in the IgG-ELISA, and 229 out of 237 (specificity: 96.6%) NAb-negative samples were also negative in the IgG-ELISA.

Neutralization assay with the VSV-based RVFV pseudotype

Virus neutralization assays using VSV pseudotype-bearing glycoproteins of viruses causing VHFs have been developed with high sensitivity and specificity.[24] In order to determine whether a VSV-based RVFV pseudotype can be applied for the screening of NAbs against RVFV infection, we produced RVFVpv and then determined whether the human sera collected from the study area could neutralize its infectivity. Single serum dilution (1:50) assay rather than titration by endpoint dilutions was performed in order to establish a high-throughput screening of NAbs. Since the infectivity of the RVFVpv, harboring the luciferase gene, could be ascertained by determining its luciferase activity, the neutralization activities of the sera were represented as the percent neutralization calculated from the reduction in the luciferase expression. Of the 278 serum samples tested, 43 (15.5%) showed more than 75% luciferase activity neutralization, and the remaining 235 (84.5%) showed less than 75% neutralization, compared with the non-serum control (Table 1). The sensitivity of the RVFVpv-based neutralization assay was determined by comparing the results with those obtained from the conventional neutralization assay using RVFV-MP12. All 34 serum samples that tested positive in the neutralization assay with RVFV-MP12 showed more than 50% neutralization of RVFVpv (Table 2). Furthermore, of the 211 serum samples that had less than 50% neutralization, none (0%) were positive for the neutralization assay with RVFV-MP12 (Table 2).

The ROC and TG-ROC analyses were performed in order to select cut-off points for the percent neutralization using RVFVpv (Figure 1). If the cut-off was defined as the intersection point of

Table 1. Summary of the results of the IgG ELISA (n=297), serum neutralization antibody (NAb) assay using VSV-RVFV-pV (n=278) and NAb assay using RVFV-MP12 (n=271) to determine seroprevalence of RVFV in humans in Borno State, Nigeria

	IgG-ELISA[a]			NAb assay	
	RVFV-rNP ELISA	LASV-rNP ELISA	CCHFV-rNP ELISA	RVFVpv NAb[b]	RVFV-MP12 NAb
No. positive (%)	42 (14.1)	22 (7.4)	7 (2.4)	43 (15.5)	34 (12.6)
No. negative (%)	255 (85.9)	275 (92.6)	290 (97.6)	235 (84.5)	237 (87.4)
Total	297 (100)	297 (100)	297 (100)	278 (100)	271 (100)

CCHFV-rNP: Crimean-Congo hemorrhagic fever virus recombinant nucleoprotein; LASV-rNP: Lassa fever virus recombinant nucleoprotein; NAb: serum neutralization antibody; RVFV: Rift Valley fever virus; RVFV-MP12: highly attenuated MP12 strain of RVFV; RVFV-rNP: RVFV recombinant nucleoprotein; RVFVpv: RVFV-glycoprotein-bearing vesicular stomatitis virus pseudotype.
[a] IgG response considered positive if the sample had a positive titer at both 1:400 and 1:1600 dilutions.
[b] >75% inhibition considered positive.

the sensitivity and specificity curves, the cut-off value was 75% neutralization, and the sensitivity and specificity were 94% and 95%, respectively. If the cut-off was defined as 50% neutralization, the sensitivity would increase to 100%, but specificity would decrease to 89% (Figure 1). There was a positive correlation between the titers of neutralizing antibodies obtained using RVFVpv and those obtained using the conventional neutralization assay with RVFV-MP12. Spearman's rank correlation coefficient (r_s) was calculated to be 0.77 (Figure 2). Thus, NAbs against RVFV can be screened by the RVFVpv-based neutralization assay using the single serum dilution format.

Table 2. The relationship between the results of the authentic virus (RVFV-MP12 strain)-based and RVFVpv-based neutralization assays (n=270)

	NAb for RVFVpv		
NAb for RVFV-MP12	% Neutralization		
	>75	50–75	<50
Positive	32 (11.9%)	2 (0.7%)	0 (0%)
Negative	11 (4.1%)	14 (5.2%)	211 (78.1%)
Total	43 (15.9%)	16 (5.9%)	211 (78.1%)

NAb: serum neutralization antibody; RVFV-MP12: highly attenuated MP12 strain of Rift Valley fever virus; RVFVpv: RVFV-glycoprotein-bearing vesicular stomatitis virus pseudotype.

Discussion

In this study, the seroprevalence of RVF was investigated among human population in Borno State, Nigeria to determine the occurrence and spread of the disease in comparison with those of Lassa fever and CCHF. Since recombinant protein-based immunoassays with high sensitivity and specificity have been demonstrated to be useful for the diagnosis of VHFs in humans,[15–17,25,26] we have used rNP-based IgG-ELISAs for the detection of serum antibodies against RVFV, LASV, and CCHFV. Of the 297 serum samples tested for RVFV-IgG, a total of 42 (14.1%) showed positive results (Table 1). The antibody prevalence observed in this study is in agreement with the results of a surveillance study carried out in the 1980s, when 14.8% of the sera collected in more than 30 locations throughout Nigeria were found to be positive for a hemagglutination-inhibiting antibody against RVFV.[11] In this study a significant difference in the prevalence of antibodies was observed (RVFV rNP-ELISA [14.1%], LASV rNP-ELISA [7.4%] and CCHFV rNP-ELISA [2.4%]), and the highest prevalence was noted for RVFV rNP-ELISA antibody. In addition, more than 12% of the samples tested had NAb activity against RVFV. These results indicate that RVFV is more actively circulating in the study area compared with LASV and CCHFV. It is therefore important to undertake a risk assessment of RVFV infection in humans in Nigeria.

RVFV is transmitted through contact with body fluids from infected humans and animals or by mosquito bites and/or aerosols. The particular location of Borno State, with its shared geographical borders with three other African countries, indicates that a regional epidemiological study should be conducted not only in the LGAs in Nigeria, but also in the neighboring countries, to identify the possible risk factors for transboundary RVFV infection. The borders are porous and unrestricted human and animal

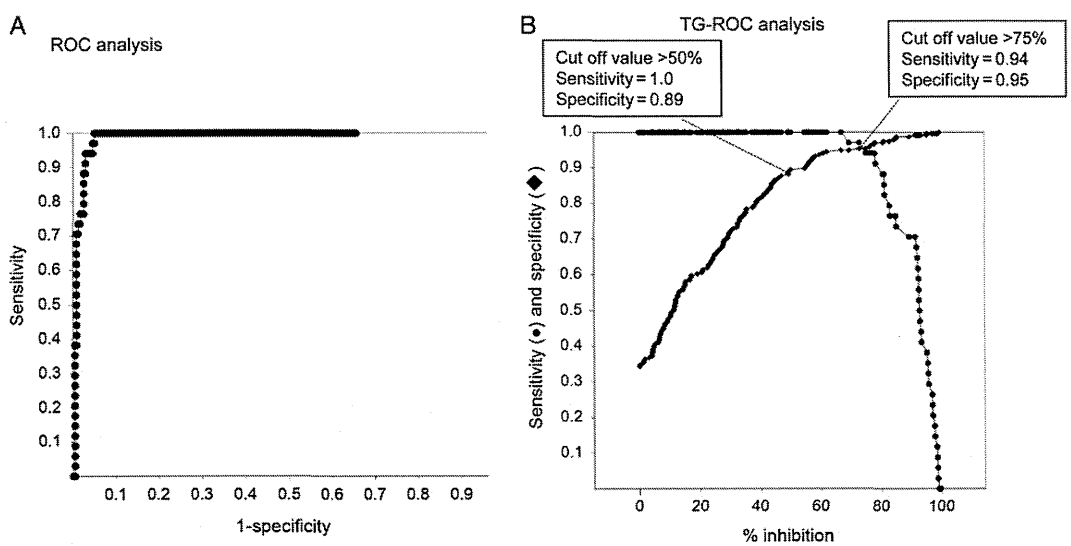

Figure 1. The results of the ROC and two-graph (TG)-ROC analyses of the vesicular stomatitis virus pseudotype virus-bearing glycoproteins of Rift Valley fever virus, (RVFVpv)-based neutralization assay. In (A) the ROC analysis graph, the specificity values are deducted from 1.0 in the x-axis, and the sensitivity vs 1-specificity data are plotted as dots. In (B) the TG-ROC analysis graph, sensitivity data are plotted as dots and specificity data are plotted as diamonds.

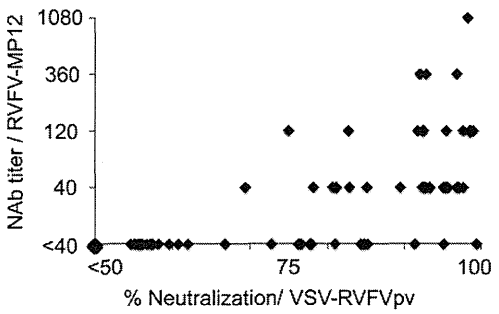

Figure 2. A comparison of the percent neutralization obtained from virus pseudotype virus-bearing glycoproteins of Rift Valley fever virus (RVFVpv)-based neutralization assay with the serum neutralization antibody (NAb) titers obtained from authentic virus (RVFV-MP12)-based neutralization assays. The data are plotted as diamonds on the scatterplot. Spearman's rank correlation coefficient (r_s) was calculated to be 0.77.

trafficking across borders is common throughout the year. In spite of the active circulation of RVFV observed in this study, no outbreak of the disease in humans or animals has been reported in the study area. This could be as a result of poor surveillance for the outbreak of the disease or a lack of expertise in disease recognition.[10,11] It is also possible that RVFV circulating in the region is a non-pathogenic strain. RVF in humans usually begins with a non-specific influenza-like acute fever, but can progress to serious hemorrhagic fever in some cases. VHFs, particularly Lassa fever, an acute viral hemorrhagic fever caused by LASV, has been reported to be endemic in Nigeria.[27,28] The symptoms of the disease also vary from a non-specific febrile illness to fatal viral hemorrhagic fever. Therefore, there is the possibility that patients with non-specific febrile illness caused by RVFV infection could be misdiagnosed with other endemic infectious diseases, such as malaria, typhoid fever or Lassa fever.

A VSV-based pseudotype system has been designed to enable the high-throughput screening of NAbs against viral infections.[29] We also developed a novel serum neutralization test using RVFVpv to detect serum antibody against RVFV. The reliability and usefulness of the assay were evaluated by comparing the results of the assay with those obtained from the widely used 'gold-standard' neutralization assay using infectious RVFV. Of the 43 serum samples that showed more than 75% neutralization by the RVFVpv-based assay, 11 were negative by the conventional RVFV-MP12 neutralization assay (Table 2). It is possible that the results of 11 negative samples were due to false-positive reactions in the VSV-RVFVpv-based assay. However, among these serum samples, one showed a higher OD_{405} value (0.443) than the cut-off OD_{405} value at 1:400 dilution, and another one was identified as a positive by the rNP-based ELISA, with OD_{405} values of 1.318 and 0.364 at the 1:400 and 1:1600 dilutions, respectively (Supplementary Table 1), indicating that the serum contained antibody to RVFV. Another possibility is that the VSV-RVFVpv-based assay was more sensitive than the standard neutralization assay using RVFV-MP12. This assumption is supported by the observation that the NAb titers measured using pseudotyped VSV bearing the GP of Nipah virus or SARS-coronavirus are higher than those obtained by using infectious viruses.[21,29,30]

The ROC and TG-ROC analyses indicated an appropriate cut-off value for the percent neutralization (75%) to demonstrate that the NAbs in the sera had high sensitivity and specificity. The conventional assay for measuring NAbs requires serial-dilutions of the test serum and takes several days for the virus to replicate to a level which results in plaque-forming or cytopathic effects in infected cells. However, the new assay based on RVFVpv uses a single serum dilution (1:50) and has a quantitative nature, where the luciferase activity can be determined one day after inoculation onto cells. Finally, pseudotyped VSVs do not produce infectious progeny viruses, thereby ensuring their safe use as diagnostic tools. Taken together, our results indicate that the RVFVpv-based assay for measuring NAb has safe, rapid and high-throughput diagnostic capabilities.

Our study has limitations, one of which is the relatively small sample size compared to the previous study, carried out in the 1980s, employing more than 3000 human sera from the different ecological zones in Nigeria.[11] In addition, we could not access detailed information on the subjects (age, profession, history of illness etc.). Although our data were obtained using the most recent serological procedures, the lack of demographic information on the study subjects makes it difficult to provide an advanced epidemiological understanding of VHFs in Nigeria. However, this study has important strengths: it provides information on RVFV infection with a high prevalence in human population in Borno State and demonstrates the usefulness of the VSV-based neutralization assay for the epidemiological investigations.

Conclusions

The results of rNP-based ELISA have shown that approximately 14% of the study population in Borno State, Nigeria, have a history of RVFV infection, and the seroprevalence of RVF was higher than those of other viral hemorrhagic fevers such as Lassa fever and CCHF. In addition, the RVFVpv-based NAb assay developed in this study has the potential to replace traditional assays based on live viruses for the diagnosis and seroepidemiological analysis of RVF in endemic and non-endemic countries.

Supplementary data

Supplementary data are available at Transactions Online (http://trstmh.oxfordjournals.org/).

Authors' contributions: DNB, FK and SSB conceived the study; SF and MS designed the study protocol; DNB, HT, TY, ST, KI and AF carried out the serological assays, and analysis and interpretation of the data. DNB and SF drafted the manuscript; MS, SM, MS and SSB critically revised the manuscript for intellectual content. All authors read and approved the final manuscript. SF and MS are guarantors of the paper.

Acknowledgements: The authors wish to thank Dr. M.A. Whitt for providing the *G-VSVΔG/luc construct. We also thank Ms. M. Ogata for her valuable assistance. The senior author (DNB) was a Visiting Scientist at the National Institute of Infectious Diseases, Tokyo, Japan, under the sponsorship of the Tertiary Education Trust Fund, Nigeria. He is also a postgraduate student in the Department of Veterinary Microbiology and Parasitology, University of Maiduguri, Nigeria.

Funding: This work was supported in part by a grant-in-aid from the Ministry of Health Labor and Welfare of Japan and the Japan Society for the Promotion of Science [H22-Shinko-Ippan-009, H22-Shinko-Ippan-006, and H25 Shinko-Ippan-004].

Competing interests: None declared.

Ethical approval: This study protocol was approved by the Borno State Ministry of Health, Nigeria and the Ethics Committee of the National Institute of Infectious Diseases, Tokyo, Japan [No. 371].

References

1 Faye O, Diallo M, Diop D et al. Rift Valley fever outbreak with East-Central African virus lineage in Mauritania, 2003. Emerg Infect Dis 2007;13:1016–23.

2 Shoemaker T, Boulianne C, Vincent MJ et al. Genetic analysis of viruses associated with emergence of Rift Valley fever in Saudi Arabia and Yemen, 2000–01. Emerg Infect Dis 2002;8:1415–20.

3 Andriamandimby SF, Randrianarivo-Solofoniaina AE, Jeanmaire EM et al. Rift Valley fever during rainy seasons, Madagascar, 2008 and 2009. Emerg Infect Dis 2010;16:963–70.

4 Archer BN, Weyer J, Paweska J et al. Outbreak of Rift Valley fever affecting veterinarians and farmers in South Africa, 2008. S Afr Med J 2011;101:263–6.

5 Gachohi JM, Bett B, Njogu et al. The 2006–2007 Rift Valley fever outbreak in Kenya: sources of early warning messages and response measures implemented by the Department of Veterinary Services. Rev Sci Tech 2012;31:877–87.

6 Heinrich N, Saathoff E, Weller N et al. High seroprevalence of Rift Valley fever and evidence for endemic circulation in Mbeya region, Tanzania, in a cross-sectional study. PLoS Negl Trop Dis 2012;6:e1557.

7 Nderitu L, Lee JS, Omolo J et al. Sequential Rift Valley fever outbreaks in eastern Africa caused by multiple lineages of the virus. J Infect Dis 2011;203:655–65.

8 Clements AC, Pfeiffer DU, Martin V, Otte MJ. A Rift Valley fever atlas for Africa. Prev Vet Med 2007;82:72–82.

9 Ezeifeka GO, Umoh JU, Belino ED, Ezeokoli CD. A serological survey for Rift Valley fever antibody in food animals in Kaduna and Sokoto States of Nigeria. Int J Zoonoses 1982;9:147–51.

10 Olaleye OD, Tomori O, Schmitz H. Rift Valley fever in Nigeria: infections in domestic animals. Rev Sci Tech 1996;15:937–46.

11 Olaleye OD, Tomori O, Ladipo MA, Schmitz H. Rift Valley fever in Nigeria: infections in humans. Rev Sci Tech 1996;15:923–35.

12 Giorgi C, Accardi L, Nicoletti L et al. Sequences and coding strategies of the S RNAs of Toscana and Rift Valley fever viruses compared to those of Punta Toro, Sicilian Sandfly fever, and Uukuniemi viruses. Virology 1991;180:738–53.

13 Bird BH, Khristova ML, Rollin PE et al. Complete genome analysis of 33 ecologically and biologically diverse Rift Valley fever virus strains reveals widespread virus movement and low genetic diversity due to recent common ancestry. J Virol 2007;81:2805–16.

14 Fafetine JM, Tijhaar E, Paweska JT et al. Cloning and expression of Rift Valley fever virus nucleocapsid (N) protein and evaluation of a N-protein based indirect ELISA for the detection of specific IgG and IgM antibodies in domestic ruminants. Vet Microbiol 2007;121:29–38.

15 Jansen van Vuren P, Potgieter AC, Paweska JT, van Dijk AA. Preparation and evaluation of a recombinant Rift Valley fever virus N protein for the detection of IgG and IgM antibodies in humans and animals by indirect ELISA. J Virol Methods 2007;140:106–14.

16 Saijo M, Georges-Courbot MC, Marianneau P et al. Development of recombinant nucleoprotein-based diagnostic systems for Lassa fever. Clin Vaccine Immunol 2007;14:1182–9.

17 Saijo M, Qing T, Niikura M et al. Recombinant nucleoprotein-based enzyme-linked immunosorbent assay for detection of immunoglobulin G antibodies to Crimean-Congo hemorrhagic fever virus. J Clin Microbiol 2002;40:1587–91.

18 Saijo M, Qing T, Niikura M et al. Immunofluorescence technique using HeLa cells expressing recombinant nucleoprotein for detection of immunoglobulin G antibodies to Crimean-Congo hemorrhagic fever virus. J Clin Microbiol 2002;40:372–5.

19 Fukushi S, Nakauchi M, Mizutani T et al. Antigen-capture ELISA for the detection of Rift Valley fever virus nucleoprotein using new monoclonal antibodies. J Virol Methods 2012;180:68–74.

20 Saijo M, Ogino T, Taguchi F et al. Recombinant nucleocapsid protein-based IgG enzyme-linked immunosorbent assay for the serological diagnosis of SARS. J Virol Methods 2005;125:181–6.

21 Fukushi S, Mizutani T, Saijo M et al. Evaluation of a novel vesicular stomatitis virus pseudotype-based assay for detection of neutralizing antibody responses to SARS-CoV. J Med Virol 2006; 78:1509–12.

22 Greiner M, Sohr D, Gobel P. A modified ROC analysis for the selection of cut-off values and the definition of intermediate results of serodiagnostic tests. J Immunol Methods 1995;185:123–32.

23 Zweig MH, Campbell G. Receiver-operating characteristic (ROC) plots: a fundamental evaluation tool in clinical medicine. Clin Chem 1993;39:561–77.

24 Fukushi S, Tani H, Yoshikawa T et al. Serological assays based on recombinant viral proteins for the diagnosis of arenavirus hemorrhagic fevers. Viruses 2012;4:2097–114.

25 Jackel S, Eiden M, Balkema-Buschmann A et al. A novel indirect ELISA based on glycoprotein Gn for the detection of IgG antibodies against Rift Valley fever virus in small ruminants. Res Vet Sci 2013;95:725–30.

26 Nakauchi M, Fukushi S, Saijo M et al. Characterization of monoclonal antibodies to Junin virus nucleocapsid protein and application to the diagnosis of hemorrhagic fever caused by South American arenaviruses. Clin Vaccine Immunol 2009;16:1132–8.

27 Ehichioya DU, Hass M, Becker-Ziaja B et al. Current molecular epidemiology of Lassa virus in Nigeria. J Clin Microbiol 2011; 49:1157–61.

28 Monath TP. Lassa fever: review of epidemiology and epizootiology. Bull World Health Organ 1975;52:577–92.

29 Kaku Y, Noguchi A, Marsh GA et al. Second generation of pseudotype-based serum neutralization assay for Nipah virus antibodies: sensitive and high-throughput analysis utilizing secreted alkaline phosphatase. J Virol Methods 2012;179:226–32.

30 Kaku Y, Noguchi A, Marsh GA et al. A neutralization test for specific detection of Nipah virus antibodies using pseudotyped vesicular stomatitis virus expressing green fluorescent protein. J Virol Methods 2009;160:7–13.

JVI
Journals.ASM.org

Analysis of Lujo Virus Cell Entry using Pseudotype Vesicular Stomatitis Virus

Hideki Tani,[a] Koichiro Iha,[a,d] Masayuki Shimojima,[a] Shuetsu Fukushi,[a] Satoshi Taniguchi,[a,d] Tomoki Yoshikawa,[a] Yoshihiro Kawaoka,[b] Naoe Nakasone,[c] Haruaki Ninomiya,[c] Masayuki Saijo,[a] Shigeru Morikawa[d]

Special Pathogens Laboratory, Department of Virology I, National Institute of Infectious Diseases,[a] Division of Virology, Department of Microbiology and Immunology, Institute of Medical Science,[b] University of Tokyo, Tokyo, Japan; Department of Biomedical Regulation, School of Health Sciences, Tottori University Faculty of Medicine, Tokyo, Japan[c]; Department of Veterinary Science, National Institute of Infectious Diseases, Tokyo, Japan[d]

ABSTRACT

Several arenaviruses are known to cause viral hemorrhagic fever (VHF) in sub-Saharan Africa and South America, where VHF is a major public health and medical concern. The biosafety level 4 categorization of these arenaviruses restricts their use and has impeded biological studies, including therapeutic drug and/or vaccine development. Due to difficulties associated with handling live viruses, pseudotype viruses, which transiently bear arenavirus envelope proteins based on vesicular stomatitis virus (VSV) or retrovirus, have been developed as surrogate virus systems. Here, we report the development of a pseudotype VSV bearing each envelope protein of various species of arenaviruses (AREpv), including the newly identified Lujo virus (LUJV) and Chapare virus. Pseudotype arenaviruses generated in 293T cells exhibited high infectivity in various mammalian cell lines. The infections by New World and Old World AREpv were dependent on their receptors (human transferrin receptor 1 [hTfR1] and α-dystroglycan [αDG], respectively). However, infection by pseudotype VSV bearing the LUJV envelope protein (LUJpv) occurred independently of hTfR1 and αDG, indicating that LUJpv utilizes an unidentified receptor. The pH-dependent endocytosis of AREpv was confirmed by the use of lysosomotropic agents. The fusion of cells expressing these envelope proteins, except for those expressing the LUJV envelope protein, was induced by transient treatment at low pH values. LUJpv infectivity was inhibited by U18666A, a cholesterol transport inhibitor. Furthermore, the infectivity of LUJpv was significantly decreased in the Niemann-Pick C1 (NPC1)-deficient cell line, suggesting the necessity for NPC1 activity for efficient LUJpv infection.

IMPORTANCE

LUJV is a newly identified arenavirus associated with a VHF outbreak in southern Africa. Although cell entry for many arenaviruses has been studied, cell entry for LUJV has not been characterized. In this study, we found that LUJpv utilizes neither αDG nor hTfR1 as a receptor and found unique characteristics of LUJV glycoprotein in membrane fusion and cell entry. Proper exclusion of cholesterol or some kinds of lipids may play important roles in LUJpv cell entry.

Arenaviruses belong to the family *Arenaviridae* and are classified into two complexes, New World and Old World arenaviruses, based on serological, genetic, and geographical relationships and the rodent hosts (1). New World arenaviruses are further divided into 3 major clades (A, B, and C). Clade B contains 5 hemorrhagic fever-causing arenaviruses that are known to cause South American hemorrhagic fever in humans: Junin virus (JUNV), Guanarito virus (GTOV), Sabia virus (SABV), Machupo virus (MACV), and Chapare virus (CHPV) (2). Of the Old World arenaviruses, Lassa virus (LASV) is endemic in western Africa and is known to cause viral hemorrhagic fever (VHF) in humans (3). Recently, another Old World arenavirus, Lujo virus (LUJV), was identified as a cause of VHF with a high case fatality rate of 80% (4).

Arenaviruses are enveloped negative-strand RNA viruses with a genome that is bisegmented into S and L segments. The S segment encodes a nucleocapsid protein (NP) and an envelope glycoprotein precursor (GPC); the L segment encodes a matrix protein (Z) and an RNA-dependent RNA polymerase (L). The GPC is synthesized as a single polypeptide and undergoes processing by the host cell signal peptidase (SPase) and subtilisin-like kexin isozyme-1/site-1-protease (SKI-1/S1P), yielding typical receptor-binding (G1), transmembrane fusion (G2), and stable signal peptide (SSP) subunits, respectively (5). Viral entry into target cells is initiated by the binding of G1 to appropriate cell surface receptors. The first cellular receptor for arenavirus to be identified was α-dystroglycan (αDG), a ubiquitous receptor for extracellular matrix proteins (6). αDG is a binding receptor for Old World arenaviruses, such as LASV and lymphocytic choriomeningitis virus (LCMV), and some of the clade C New World arenaviruses (7). Among the New World arenaviruses, many pathogenic viruses use human transferrin receptor 1 (hTfR1) as a receptor for cell entry (8, 9). A number of additional receptor candidates for JUNV, LASV, and LCMV have recently been reported, including the C-type lectin family, dendritic cell-specific intercellular adhesion molecule 3-grabbing nonintegrin (DC-SIGN), liver and lymph node sinusoidal endothelial calcium-dependent lectin (LSECtin), and two members of the TAM family (Axl and Tyro3)

Received 24 February 2014 Accepted 8 April 2014
Published ahead of print 16 April 2014
Editor: D. S. Lyles
Address correspondence to Shigeru Morikawa, morikawa@nih.go.jp.

doi:10.1128/JVI.00512-14

(10–13). In the case of LUJV, the receptor candidate (or candidates) is at this time largely unknown.

The categorization in many countries of VHF-causing arenaviruses as biosafety level 4 (BSL4) pathogens means that they may only be handled in specific institutions that are equipped with BSL4 facilities. This has impeded analysis of the life cycle and pathogenesis of these pathogenic arenaviruses and the development of therapeutic agents and vaccines for arenaviral hemorrhagic fevers. The analysis of the initial steps of viral infection, including identification of the entry receptors, is important for understanding the life cycle of these viruses and for further developing entry inhibitors. Several alternative research tools for the viruses have therefore been developed. A cell fusion assay was established to examine the membrane fusion activities of viral envelope proteins (14). The assay is sensitive and can easily determine cell fusion using reporter genes. Pseudotype virus systems based on vesicular stomatitis virus (VSV) or lentivirus and retrovirus have also been established to examine viral entry mechanisms and to identify putative entry receptors (15). These systems are beneficial in the study of highly pathogenic arenavirus infections.

In the present study, we generated pseudotype VSVs bearing envelope proteins of several arenaviruses, including LUJV. In particular, the characteristics of envelope proteins of LUJV were determined for the first time with respect to their glycosylation, fusion activities, and utilization of known arenaviral receptors and the involvement of cholesterol or sphingolipid in cell entry.

MATERIALS AND METHODS

Plasmids and cells. The cDNAs of the SABV, MACV, CHPV, and LUJV GPCs were obtained by chemical synthesis (Codon Devices, Cambridge, MA). The GPC cDNAs of JUNV (strain MC2) and LASV (strain Josiah) were supplied by V. Romanowski (Universidad Nacional de La Plata) and C. J. Peters (University of Texas Medical Branch), respectively. The GenBank accession numbers of the nucleotide sequences of the SABV, MACV, CHPV, LUJV, JUNV, and LASV GPC genes are NC_006317, NC_005078, NC_010562, FJ952384, U70799, and J04324, respectively. The GPC cDNAs of SABV, MACV, CHPV, LUJV, JUNV, and LASV were cloned into the expression vector pKS336 (16). The resulting plasmids were designated pKS-SABV-GP, pKS-MACV-GP, pKS-CHPV-GP, pKS-LUJV-GP, pKS-JUNV-GP, and pKS-LASV-GP. Each GP sequence of the plasmids was confirmed to be identical to the original cDNA sequence using an ABI Prism 3100-Avant Genetic Analyzer (Applied Biosystems). The plasmid pKS-EBOV-GP (Reston) was prepared as described previously (17).

FLAG/One-STrEP (FOS)-tagged fusion protein expression vectors were also constructed. cDNAs of the CHPV-GP, LUJV-GP, JUNV-GP, and LASV-GP with the stop codon deleted were synthesized by PCR from each of the above-described cDNAs. The PCR products were cloned into pCAG-MCS2-FOS, which expresses carboxyl-terminally FOS-tagged fusion protein (provided by E. Morita, Osaka University). The resulting plasmids were designated pCAG-CHPV-GP-FOS, pCAG-LUJV-GP-FOS, pCAG-JUNV-GP-FOS, and pCAG-LASV-GP-FOS. The cDNA encoding G protein (G) of VSV was amplified from pCAG-VSV-G by PCR and cloned into pCAG-MCS2-FOS to construct pCAG-VSV-G-FOS in order to express carboxyl-terminally FOS-tagged VSV G protein.

A plasmid carrying hTfR1 cDNA was generated. Total RNAs were isolated from 293T cells using TRIzol Reagent (Invitrogen, Carlsbad, CA) according to the manufacturer's instructions. The cDNA was synthesized by reverse transcription with Superscript III reverse transcriptase (Invitrogen) using random hexamer primers (Invitrogen). The cDNA encoding hTfR1 was amplified by PCR using an Expand High Fidelity PCR System (Roche Applied Science, Indianapolis, IN) with cDNA synthesized from the 293T RNAs. The amplified cDNA was cloned into pKS336. The resulting plasmid was designated pKS-hTfR1. The cloned sequence was confirmed to be identical to the hTfR1 cDNA sequence using an ABI Prism 3100-Avant Genetic Analyzer.

Hamster (BHK and CHO), mouse (NIH 3T3, NMuLi, and P388), rabbit (PK15), monkey (VeroE6, COS7, and MARC), and human (Huh7, HepG2, Hep3B, 293T, HeLa, Saos-2, Raji, U937, Molt-4, and Jurkat) cell lines were obtained from the American Type Culture Collection (Manassas, VA) or DS Pharma Biomedical Co. Ltd. (Osaka, Japan). All of the cell lines, with the exceptions of Raji, Molt-4, P388, and Jurkat cells, were grown in Dulbecco's modified Eagle's medium (DMEM) (Sigma-Aldrich, St. Louis, MO) containing 10% heat-inactivated fetal bovine serum (FBS). Raji, Molt-4, P388, and Jurkat cells were grown in RPMI 1640 (Sigma-Aldrich) containing 10% FBS. To establish a CHO cell line that stably expresses hTfR1 (CHO/hTfR1), CHO cells were transfected with pKS-hTfR1 using Fugene HD (Roche) reagent. The transfected CHO cells were selected with DMEM containing 10% FBS and 2 μg/ml of Blasticidin S-HCl (Invitrogen). When clusters of the cells appeared, some clusters of the cells were cloned and subcultured to establish CHO/hTfR1. The αDG knockout embryonic stem (ES) cell clone 354.B11 was provided by K. P. Campbell (Howard Hughes Medical Institute, University of Iowa) and was cultured using Esgro Complete Plus Clonal Grade Medium (Merck Millipore, Darmstadt, Germany). A CHO cell mutant defective in the NPC1 gene (CHO/A101) and CHO/A101 cells stably expressing FLAG-tagged NPC1 (CHO/A101/NPC1-KI) had been previously generated and were maintained in Ham's F-12 containing 10% FBS (18).

Generation of pseudotype VSVs. Pseudotype VSVs bearing the GPC of arenaviruses (AREpv), GP of ebolavirus (EBOpv), G of VSV (VSVpv), and murine leukemia virus envelope protein (MLVpv) were generated as described previously (17, 19, 20). Briefly, 293T cells were grown to 70% confluence on collagen-coated tissue culture plates and then transfected with pKS-LASV-GP, pKS-JUNV-GP, pKS-LUJV-GP, pKS-CHPV-GP, pKS-SABV-GP, pKS-MACVGP, pKS-EBOV-GP, pCAG-CHPV-GP-FOS, pCAG-LUJV-GP-FOS, pCAG-JUNV-GP-FOS, pCAG-LASV-GP-FOS, pCAG-VSV-G, pCAG-VSV-G-FOS, or pFBASALF (which expresses murine leukemia virus envelope proteins; provided by T. Miyazawa, Kyoto University). After 24 h of incubation, the transfected cells were infected with G-complemented (*G) VSVΔG/Luc (*G-VSVΔG/Luc) (21) at a multiplicity of infection (MOI) of 0.1. The virus was adsorbed and then extensively washed four times with serum-free DMEM. After 24 h of incubation, the culture supernatants containing pseudotype VSVs were centrifuged to remove cell debris and stored at −80°C until use. The infectious titers of the pseudotype VSVs were also determined by a focus-forming assay, as described below, and were measured as focus-forming units (FFU). AREpv, EBOpv, VSVpv, and MLVpv infectivities were assessed by luciferase activity. The relative light unit (RLU) value of luciferase was determined using a Bright-Glo luciferase assay system (Promega Corporation, Madison, WI), according to the manufacturer's protocol.

Focus-forming assay. Huh7 or Vero cells were transfected with pCAG-VSV-G. At 24 h posttransfection, the cells infected with the pseudotype viruses were cultured with 0.8% methylcellulose in 10% FBS DMEM for 48 h. FFU were determined by counting visible foci.

Immunofluorescence assays. For immunofluorescence staining of the cells with antibodies, Huh7 cells transfected with pCAG-LASV-GP-FOS, pCAG-JUNV-GP-FOS, pCAG-LUJV-GP-FOS, pCAG-CHPV-GP-FOS, or pCAG-VSV-G-FOS or CHO/hTfR1 cells were fixed with acetone at room temperature for 5 min. To stain the FOS-tagged protein and hTfR1, the fixed transfected Huh7 and CHO/hTfR1 cells were incubated with mouse monoclonal anti-FLAG primary antibody (Sigma) and mouse monoclonal anti-hTfR1 antibody (BD Biosciences, San Jose, CA), respectively. The CHO cells were also prepared and stained as hTfR1 negative-control cells. All of the cells were rinsed with phosphate-buffered saline (PBS) and incubated with goat anti-mouse Alexa Fluor 488 (Invitrogen). After washing with PBS, the stained cells were observed under a fluorescence microscope (BZ-9000; Keyence, Osaka, Japan).

Immunoblotting. 293T cells were transfected with each of the plasmids pCAG-CHPV-GP-FOS, pCAG-LUJV-GP-FOS, pCAG-JUNV-GP-FOS, pCAG-LASV-GP-FOS, and pCAG-VSV-G-FOS. At 24 h posttransfection, the cells were collected and lysed in PBS containing 1% NP-40. The lysates were centrifuged to separate insoluble pellets from supernatants. The supernatants were used as samples. Pseudotype VSVs bearing FOS-tagged GPCs generated as described above were pelleted through a 20% (wt/vol) sucrose cushion at 25,000 rpm for 2 h in an SW28 rotor (Beckman Coulter, Tokyo, Japan). The pellets were resuspended in PBS and used as additional samples. Each sample, boiled in loading buffer, was subjected to 10% sodium dodecyl sulfate-polyacrylamide gel electrophoresis (SDS-PAGE). The proteins were electrophoretically transferred to a methanol-activated polyvinylidene difluoride (PVDF) membrane (Millipore, Billerica, MA) and reacted with mouse monoclonal anti-FLAG antibody (Sigma). Immune complexes were visualized with SuperSignal West Dura Extended Duration Substrate (Pierce, Rockford, IL) and detected by an LAS3000 analyzer (Fuji Film, Tokyo, Japan).

The lysates of CHO/hTfR1 and CHO cells were also treated as described above. To detect the bands of hTfR1 and β-actin, mouse monoclonal anti-hTfR1 antibody (BD Biosciences) and mouse monoclonal anti-β-actin antibody (Sigma), respectively, were used as described above.

Effects of treatment with antiserum on LUJpv infectivity. To characterize the infection of LUJpv, the pseudotype was preincubated with serially diluted anti-LUJV-GP polyclonal antibody for 1 h at 37°C and then inoculated into Huh7 cells. Anti-LUJV-GP polyclonal antibody was prepared by immunization of rabbits with the expression plasmid pKS-LUJV-GP, as described previously (22). After 2 h of adsorption at 37°C, the cells were washed with DMEM containing 10% FBS, and infectivity was determined after 24 h of incubation at 37°C.

Involvement of hTfR1 in AREpv infections. To determine the involvement of hTfR1 in viral entry, Huh7 or U937 cells were pretreated with various concentrations of anti-hTfR1 for 1 h at 37°C and inoculated with a series of AREpv, VSVpv, or MLVpv at an MOI of 1. After 1 h of adsorption at 37°C, the cells were washed and cultured for 24 h at 37°C. Pseudotype infectivities were determined by measuring luciferase activities after 24 h of incubation at 37°C.

The CHO and CHO/hTfR1 cells were infected with a series of AREpv or VSVpv, respectively, at an MOI of 1. Pseudotype infectivities were determined by measuring luciferase activities after 24 h of incubation at 37°C. AREpv infectivity for CHO/hTfR1 cells was normalized to the infectivity for CHO cells.

Huh7 cells were incubated at 37°C for 2 h in the presence of various concentrations of ferric ammonium citrate (FAC), which is rich in iron and is known to decrease TfR mRNA in the cells (23). The cells were then infected with the series of AREpv or VSVpv, as described above. Pseudotype infectivities were determined by measuring luciferase activities after 24 h of incubation at 37°C.

Involvement of αDG in AREpv infection. To examine the involvement of αDG in viral entry, Raji, Jurkat, or αDG knockout ES cells expressing like-acetylglucosaminyltransferase (LARGE) or αDG were prepared by infection with lentiviral vectors encoding LARGE, DG, or control (fCD2) genes as constructed previously (11). The cells were infected with a series of AREpv or VSVpv at an MOI of 1. Pseudotype infectivities were determined by measuring luciferase activities after 24 h of incubation at 37°C.

Effects of enzymes, chemicals, and low-pH exposure on AREpv infection. To examine the effects of oligosaccharide modification of arenavirus GPs or VSV-G, cell lysates and purified pseudotype virions were digested with endoglycosidase H (Endo H) or peptide-*N*-glycosidase F (PNGase F) (Roche) in accordance with the manufacturer's protocol and analyzed by immunoblotting.

To examine the effects of endosomal acidification of cells on viral entry, Huh7 cells were treated with various concentrations of inhibitors of endosomal acidification—bafilomycin A_1 from *Streptomyces griseus* (Sigma), ammonium chloride (Sigma), and chloroquine (Sigma)—for 1 h at 37°C. The cells were then infected with the series of AREpv, VSVpv, or MLVpv at an MOI of 1. Pseudotype infectivity was determined by measuring luciferase activities after 24 h of incubation at 37°C.

To examine the pH dependence of AREpv cell entry, the series of AREpv or VSVpv was exposed to citrate-phosphate buffer (0.1 M citric acid, 0.2 M sodium dihydrogenorthophosphate) adjusted to the indicated pH level (pH 7, 6, 5, 4, or 3) for the indicated time (0, 15, 30, 60, 90, or 120 s). After pH neutralization with a 100× volume of DMEM containing 10% FBS, the viruses were inoculated into Huh7 cells. After 24 h of incubation at 37°C, residual infectivity was determined by measuring luciferase activities and comparison with the infectivities of the pseudotypes exposed to the buffer adjusted to pH 7.

To examine the involvement of cholesterol and sphingolipids in viral entry, Huh7 cells were treated with various concentrations of chlorpromazine, imipramine, desipramine, amitriptyline, or U18666A for 1 h at 37°C. The cells were then infected with the series of AREpv, EBOpv, VSVpv, or MLVpv at an MOI of 1. Pseudotype infectivity was determined by measuring luciferase activities after 24 h of incubation at 37°C.

To examine the involvement of NPC1 in viral entry, wild-type CHO (CHO/wt), CHO/A101, and CHO/A101/NPC1-KI cells were infected with the series of AREpv, EBOpv, or VSVpv at an MOI of 1. Pseudotype infectivity for these cells was determined by measuring luciferase activities after 24 h of incubation at 37°C. Pseudotype infectivity for CHO/A101 and CHO/A101/NPC1-KI cells was normalized to the infectivity for CHO/wt cells.

Syncytium formation and quantitative reporter assays for cell fusion. To examine whether syncytium formation of the cells expressing arenavirus GPC is induced by low-pH exposure, Huh7 cells were transfected with pCAG-CHPV-GP-FOS, pCAG-LUJV-GP-FOS, pCAG-JUNV-GP-FOS, pCAG-LASV-GP-FOS, or pCAG-VSV-G-FOS. At 24 h posttransfection, the cells were rinsed once with PBS and then incubated with citrate-phosphate buffers adjusted to the indicated pH value (pH 7, 6, 5, 4, or 3) for 2 min. The citrate-phosphate buffers were then replaced with DMEM containing 10% FBS and incubated for 24 h for LASV-GP/JUNV-GP- and LUJV-GP/CHPV-GP-expressing cells or 8 h for VSV-G-expressing cells. The cell monolayers were then observed for the induction of cell fusion under a phase-contrast microscope.

To quantify cell fusion induced by arenavirus GPs, a reporter assay was carried out as follows. 293T cells were grown on 35-mm tissue culture plates and transfected with pCAG-CHPV-GP-FOS, pCAG-LUJV-GP-FOS, pCAG-JUNV-GP-FOS, pCAG-LASV-GP-FOS, or pCAG-VSV-G-FOS, together with pCAGT7pol (provided by Y. Matsuura, Osaka University), an expression plasmid carrying the T7 RNA polymerase gene under the control of the CAG promoter (14). The Huh7 target cells were grown on 35-mm tissue culture plates and transfected with pT7EMCVLuc (provided by Y. Matsuura), a reporter plasmid carrying a firefly luciferase gene under the control of the T7 promoter. At 24 h posttransfection, the target cells were collected by trypsinization and regrown in a 96-well plate. The 293T cells were treated with 0.05% EDTA in PBS and suspended in DMEM containing 10% FBS. The 293T cells were overlaid onto the target Huh7 cells and incubated for 4 h. The cocultured cells were bathed in citrate-phosphate buffers adjusted to the indicated pH values for 2 min and then incubated with DMEM containing 10% FBS for 12 h. Cell fusion activity was quantitatively determined by measuring luciferase gene expression in the lysates of the cocultured cells. The RLU values of luciferase were determined using a Bright-Glo luciferase assay system and normalized to the values of cells treated with pH 7 buffer.

RESULTS

Production and characterization of AREpv. LASpv, JUNpv, LUJpv, CHPpv, and VSVpv were generated in 293T cells transiently expressing the carboxyl-terminally FOS-tagged envelope glycoproteins of LASV, JUNV, LUJV, CHAPV, and VSV, respectively, upon infection of *G pseudotype VSV, as previously reported (21, 24). To examine the properties of the arenaviral GPs

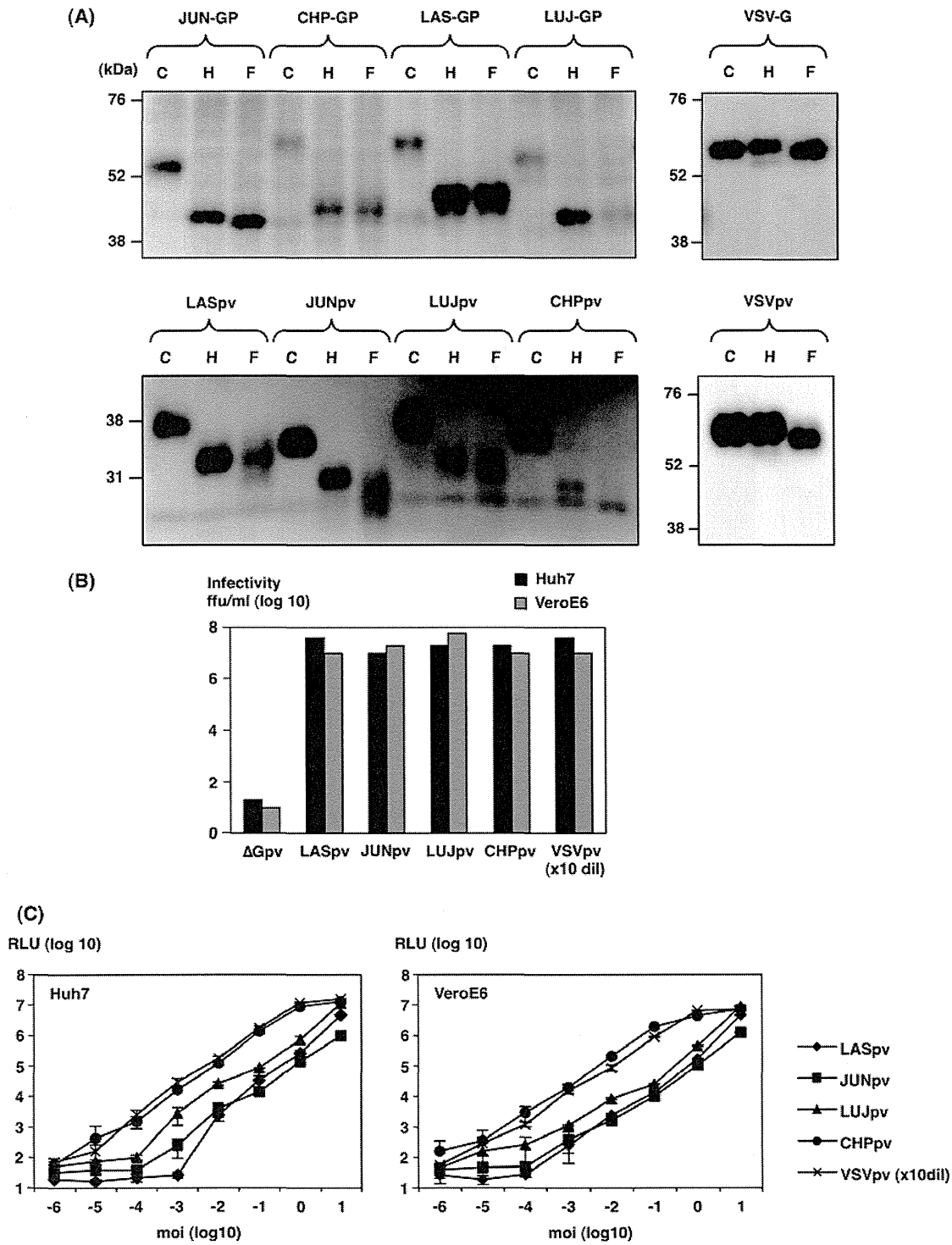

FIG 1 Glycosylation of glycoproteins in AREpv. (A) The GPC or G2 proteins of arenaviruses (LAS-GP, JUN-GP, LUJ-GP, and CHP-GP) or G protein of VSV expressed in 293T cells (top) and incorporated into the particles of AREpv (LASpv, JUNpv, LUJpv, and CHPpv) or VSVpv (bottom) were either untreated (lanes C) or treated with endoglycosidase H (lanes H) or peptide-*N*-glycosidase F (lanes F). Following fractionation on SDS-PAGE gels, the glycoproteins were detected by immunoblotting using anti-FLAG monoclonal antibody. (B) Infectivities of AREpv generated in 293T cells were determined in Huh7 and VeroE6 cells by focus-forming assay. (C) Dose-(MOI)-dependent relative luciferase activities (RLU) were determined in Huh7 and VeroE6 cells by luciferase assay. The MOI of each virus was determined on the basis of the titer in a focus-forming assay in Huh7 cells. The results shown are from three independent assays, with error bars representing standard deviations. VSV without envelope (ΔG) was used as a negative control. VSVpv (VSV) was used at 10-fold dilution (dil).

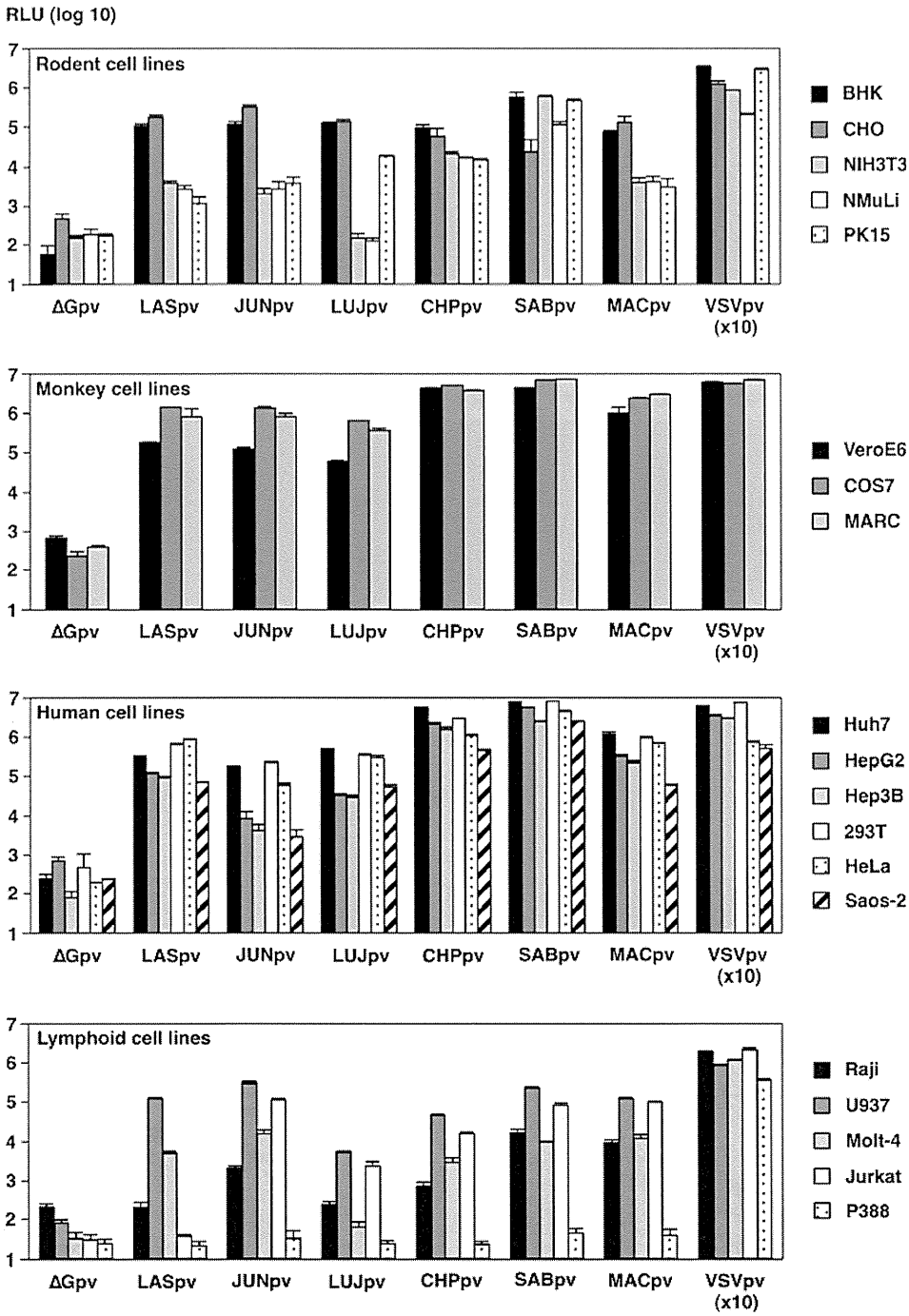

FIG 2 Efficiency of gene transduction into various mammalian cell lines by AREpv. The AREpv (LASpv, JUNpv, LUJpv, CHPpv, SABpv, and MACpv) generated by 293T cells were inoculated into the indicated cell lines at an MOI of 1. The MOI of each virus was determined on the basis of the titer in a focus-forming assay in Huh7 cells. At 24 h postinfection, the infectivities of the viruses were determined as RLU. The results shown are from three independent assays, with error bars representing standard deviations. ΔG was used as a negative control, and VSV was used at 10-fold dilution.

incorporated into AREpv particles, the arenaviral GPs expressed in 293T cells and incorporated into the viral particles were digested with Endo H and PNGase F and then examined by immunoblotting using anti-FLAG monoclonal antibody (Fig. 1A). Since the arenaviral GPCs were FOS tagged at the carboxyl terminus, the GPC and processed G2 were detected in the immunoblotting. All of the GPCs in the lysates of the cells transfected with GPC-expressing plasmids and G2 incorporated into the viral particles that were examined in the present study were sensitive to both Endo H and PNGase F treatments, suggesting that both immature and mature GPs exhibited high-mannose-type glycosylation. In contrast, the sugar chains of VSV-G protein in the cells and on the

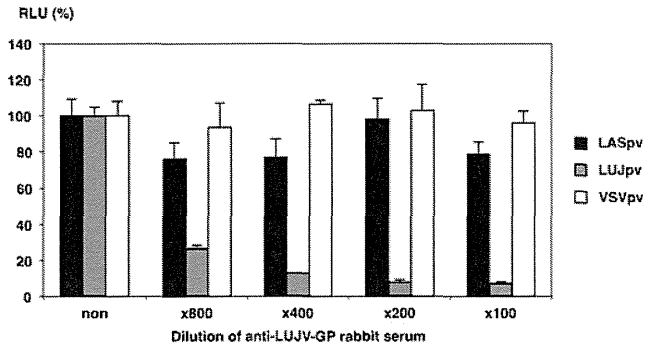

FIG 3 Neutralization of AREpv infection by Lujo virus GP antibody. Shown is the effect of anti-LUJ-GP rabbit serum on the infectivity of LASpv, LUJpv, and VSVpv for Huh7 cells. The viruses were preincubated for 1 h at room temperature with the indicated dilution of antibody before infection of Huh7 cells. Luciferase activities were determined at 24 h postinfection. The results shown are from three independent assays, with error bars representing standard deviations.

virions were sensitive to PNGase F but resistant to Endo H, indicating that the sugar chains of VSV-G protein were modified to the complex- or hybrid-type glycans, which is consistent with previous reports (25, 26) (Fig. 1A).

To evaluate the correlation of infectious titers and luciferase activities in AREpv infection, a focus-forming assay was performed (Fig. 1B). VSV lacking an envelope protein (ΔGpv) was used as a negative control. The infectious titers of all of the AREpv were shown to be high ($\sim 1 \times 10^7$ to 5×10^7 IU/ml) on both Huh7 and VeroE6 cells. The luciferase activities of all of the AREpv-infected cells were correlated with the MOI (Fig. 1C).

To further examine AREpv infectivity for various mammalian cell lines, LASpv, JUNpv, LUJpv, CHPpv, SABpv, and MACpv were inoculated into the indicated cell lines (Fig. 2). Almost all of the cell lines were susceptible to AREpv infection. Among them, COS7, MARC, Huh7, 293T, and HeLa cells were highly susceptible to AREpv infection, followed by BHK, CHO, VeroE6, HepG2, Hep3B, Saos-2, and U937. Other cell lines, NIH 3T3, NMuLi, PK15, Raji, Molt-4, and Jurkat cells, were less susceptible to infection by many of the AREpv, while P388 showed no susceptibility to AREpv infection. It is noteworthy that NIH 3T3, NMuLi, and Molt-4 cells or Jurkat cells were not susceptible to infection with LUJpv or LASpv, respectively. To determine the specificity of infection of LUJpv, neutralization assays of the pseudotypes were performed using anti-LUJV-GP rabbit serum. The infectivity of LUJpv, but not that of LASpv and VSVpv, for Huh7 cells was clearly inhibited by anti-LUJV-GP rabbit serum in a dose-dependent manner (Fig. 3). These data indicated that LUJpv infection exhibited GP-mediated entry.

Entry pathways of the AREpv. Previous studies showed that infections by LASV, JUNV, and some other arenaviruses were inhibited by treatment with lysosomotropic agents, such as ammonium chloride or bafilomycin A_1, suggesting that arenaviruses enter target cells via pH-dependent endocytosis (27–29). To examine the pH-dependent entry pathway of the AREpv, Huh7 cells were pretreated with various concentrations of bafilomycin A_1, ammonium chloride, or chloroquine, and then the cells were inoculated with a series of AREpv, VSVpv, and MLVpv (Fig. 4). As expected, the treatment of the cells with these reagents did not affect the infectivity of MLVpv, which enters cells through a pH-independent direct fusion of the viral membrane and plasma membrane. In contrast, infections of all of the AREpv and VSVpv, which enter cells through pH-dependent endocytosis, were inhibited by treatment of the cells with all of the aforementioned reagents in a dose-dependent manner. This result suggests that AREpv enter cells through pH-dependent endocytosis. It is noteworthy that treatment of cells with chloroquine dramatically reduced the infectivity of LUJpv, even at lower concentrations, while the infectivities of CHPpv and SABpv were slightly reduced with higher concentrations of chloroquine (Fig. 4C).

Involvement of TfR1 in AREpv infection. Among the candidates for cellular receptors for arenaviruses, hTfR1 was shown to be the principal receptor for the infection of New World clade B arenaviruses. It is not known whether LUJV exhibits hTfR1-dependent infection. To determine the involvement of hTfR1 in AREpv infection, Huh7 or U937 cells were pretreated with anti-hTfR1 monoclonal antibody and infected with the pseudotypes. JUNpv, CHPpv, SABpv, and MACpv infections in Huh7 and U937 cells were inhibited by anti-hTfR1 monoclonal antibody in a dose-dependent manner, whereas no inhibition of infection was observed with LASpv, LUJpv, or VSVpv (Fig. 5A). To further confirm the involvement of hTfR1, infectivities of AREpv for CHO cells stably expressing hTfR1 were examined. The expression of hTfR1 was confirmed by immunofluorescence assay and immunoblotting (Fig. 5B) (24). The expression of hTfR1 in CHO cells conferred increased susceptibility to JUNpv, CHPpv, SABpv, and MACpv infection, but not to LASpv, LUJpv, or VSVpv infection (Fig. 5C). FAC is known to downregulate TfR1 expression and inhibit infection by pseudotype viruses of the New World arenaviruses (9). In this study, infections by pseudotype viruses of the New World arenaviruses, namely, JUNpv, CHPpv, SABpv, and MACpv, were inhibited by FAC treatment (Fig. 5D). Infections by LASpv and VSVpv, which do not utilize hTfR1 as a receptor, were not affected by FAC treatment (Fig. 5D). It is noteworthy that infection with LUJpv was also inhibited by FAC treatment. These results suggest that LUJV does not utilize hTfR1 as a receptor but utilizes an unknown receptor, which is affected by FAC treatment. The results of the present study confirmed TfR1-dependent entry in New World arenavirus infections. In contrast, LUJpv and LASpv infections exhibited TfR1-independent entry.

Involvement of αDG in AREpv infection. To further examine the involvement of another arenavirus receptor candidate, αDG, in arenavirus infection, a series of AREpv were inoculated into LARGE-expressing Raji and Jurkat cells. LARGE is a putative *N*-acetylglucosaminyltransferase whose expression compensates for any lack of O-mannosylation of DG (30). Expression of O-mannosylated DG in these cells was examined as previously described (reference 11 and data not shown). The expression of LARGE in both Raji and Jurkat cells conferred susceptibility to LASpv infection, but not to JUNpv, LUJpv, CHPpv, or VSVpv infection (Fig. 6A). To further confirm this result, the infectivities of AREpv were examined in DG knockout ES cells transfected with DG-expressing or control plasmids. The expression of DG in the DG knockout ES cells resulted in an increase in LASpv infection, whereas no significant increases were observed in the other pseudotype infections (Fig. 6B). These results confirmed that LASpv exhibited αDG-dependent cell entry, while LUJpv and New World AREpv infections exhibited αDG-independent cell entry.

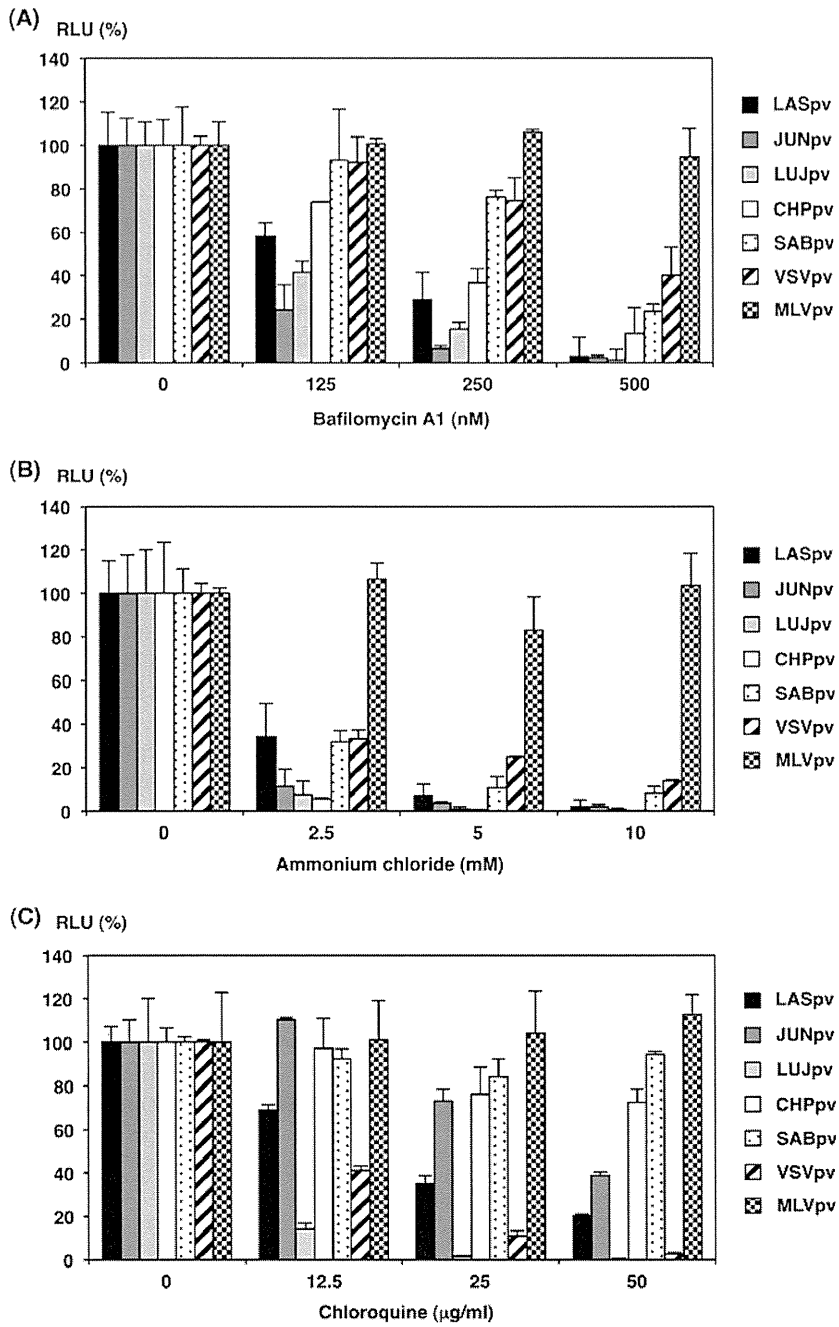

FIG 4 Inhibition of AREpv infection by H^+-ATPase inhibitors. AREpv (LASpv, JUNpv, LUJpv, CHPpv, and SABpv), VSVpv, and MLVpv were inoculated into Huh7 cells after treatment with various concentrations of bafilomycin A_1 (A), ammonium chloride (B), or chloroquine (C). Luciferase activities were determined at 24 h postinfection. The results shown are from three independent assays, with error bars representing standard deviations.

Syncytium formation and cell fusion activity in cells expressing arenaviral GPs. To examine syncytium formation in the arenaviral-GP-expressing cells, Huh7 cells were transfected with expression plasmids encoding various arenaviral GPs or VSV-G and cultured for 24 h. The cells were then treated with the indicated pH buffer for 2 min. The expression of each viral GP was confirmed by immunofluorescence assay with anti-FLAG antibody 24 h after the transfection of the expression plasmids. Synctia were observed after treatment with buffer at pH 4 in LASV-GP-expressing cells, below pH 5 in JUNV-GP- and CHPV-GP-expressing cells, and below pH 6 in VSV-G-expressing cells. In contrast, no syncytium formation was observed in LUJV-GP-expressing cells, even by treatment with buffer at pH 4 (Fig. 7A).

To further examine cell fusion activities of the arenaviral GPs, we utilized a previously established, highly sensitive, and quantitative reporter gene activation method (14). Cell fusion was induced in LASV-GP-expressing cells below pH 4, in JUNV-GP- and CHPV-GP-expressing cells below pH 5, and in VSV-G-ex-

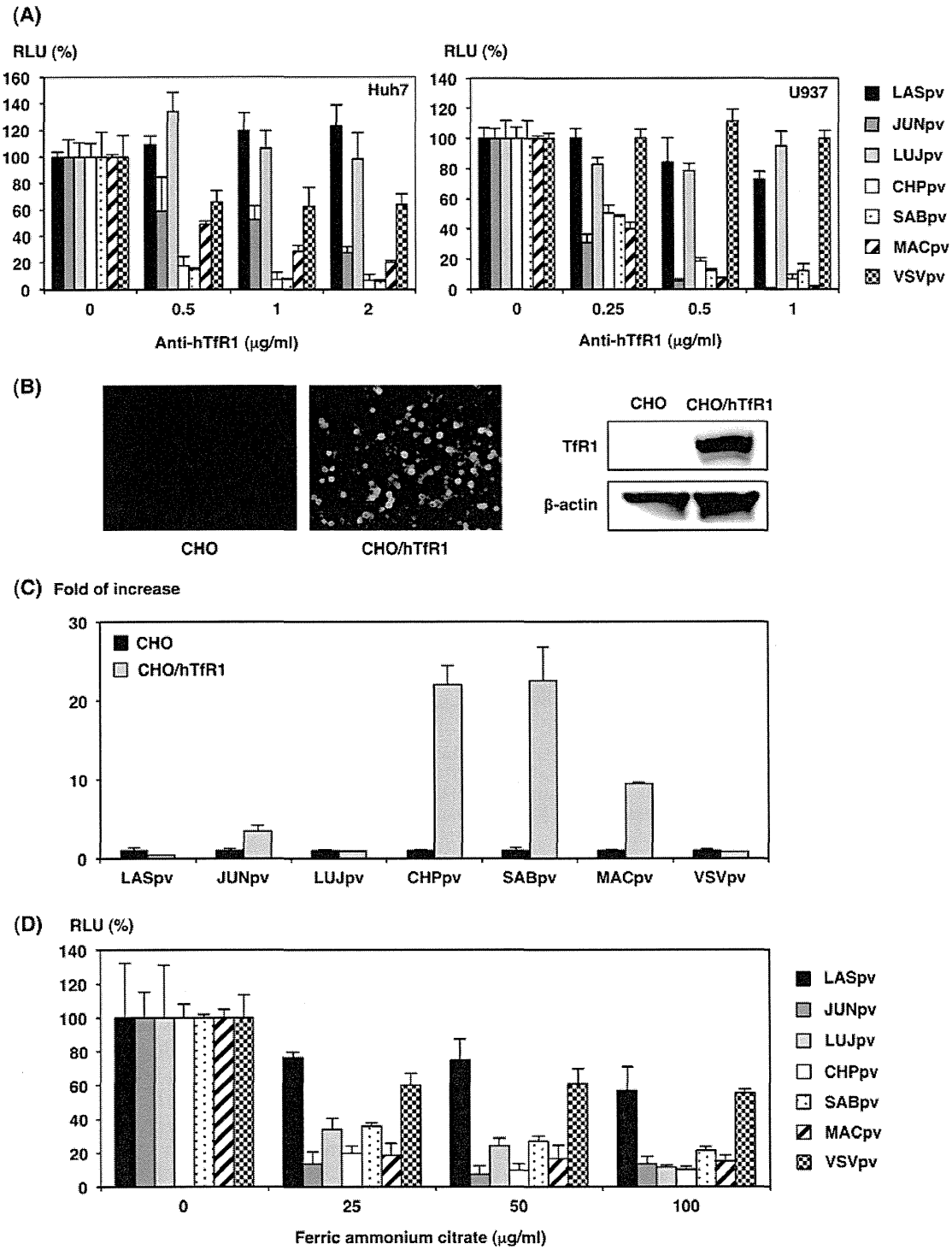

FIG 5 Involvement of human TfR1 in AREpv infection. (A) Inhibition of AREpv infection by anti-hTfR1 antibody. Huh7 or U937 cells were pretreated with various concentrations of anti-hTfR1 antibody for 1 h and inoculated with LASpv, JUNpv, LUJpv, CHPpv, SABpv, MACpv, or VSVpv, and infectivities were determined at 24 h postinfection by measuring luciferase activity. (B) Expression of hTfR1 on CHO cell lines constitutively expressing hTfR1 (CHO/hTfR1) was examined by immunofluorescence assay (left) or immunoblotting assay (right). (C) Infectivities of pseudotype immunoviruses for CHO cells expressing hTfR1. CHO or CHO/hTfR1 cells were infected with LASpv, JUNpv, LUJpv, CHPpv, SABpv, MACpv, or VSVpv, and infectivities were determined at 24 h postinfection by measuring luciferase activities. The infectivities of AREpv for CHO/hTfR1 cells were normalized to the infection of parental CHO cells. (D) Huh7 cells were pretreated with the indicated concentration of FAC and incubated at 37°C. After 1 h of incubation, the cells were inoculated with LASpv, JUNpv, LUJpv, CHPpv, SABpv, MACpv, or VSVpv, and infectivities were determined at 24 h postinfection by measuring luciferase activities. The results shown are from three independent assays, with error bars representing standard deviations.

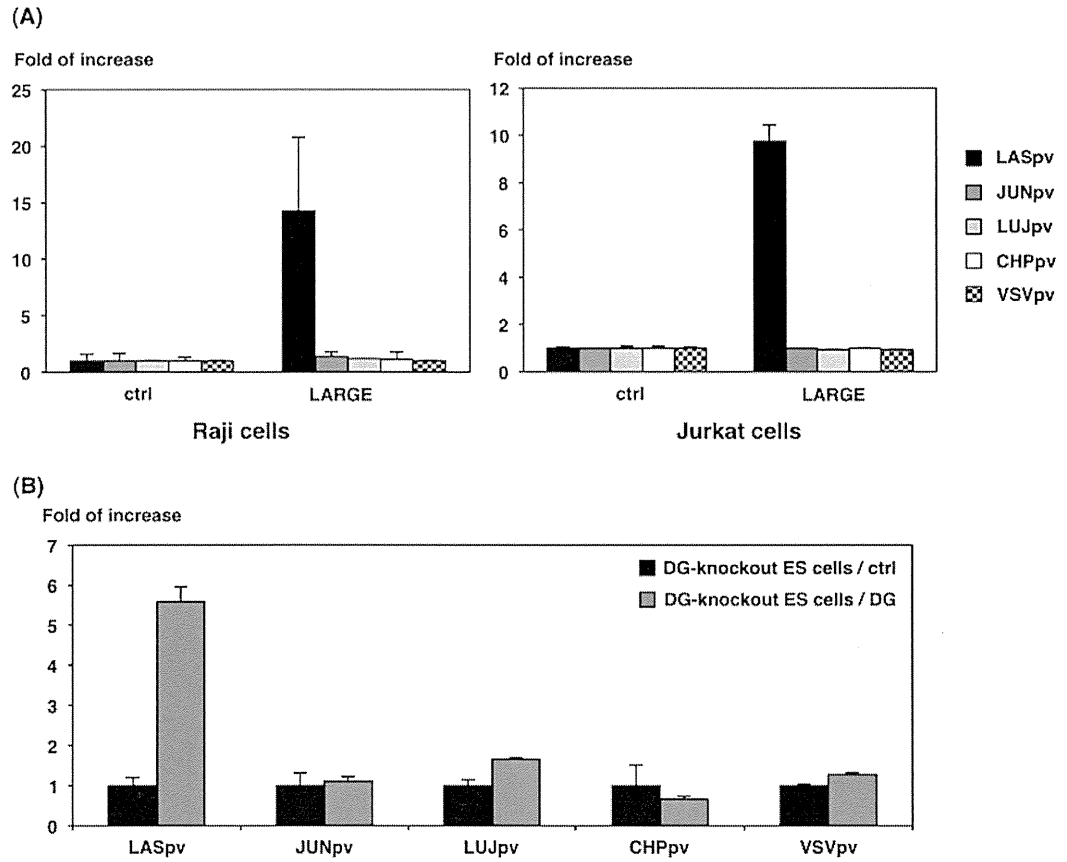

FIG 6 Involvement of αDG in AREpv infection. (A) Infectivities of AREpv in Jurkat or Raji cells expressing LARGE. Raji and Jurkat cells were transfected with the plasmid encoding LARGE or empty vector (ctrl). (B) Infectivities of AREpv in DG knockout ES cells expressing αDG. DG knockout ES cells were transfected with the plasmid encoding αDG or empty vector (ctrl). At 24 h posttransfection, the cells were infected with LASpv, JUNpv, LUJpv, CHPpv, or VSVpv, and infectivities were determined by measurement of luciferase activities. The results shown are from three independent assays, with error bars representing standard deviations.

pressing cells below pH 6. Cell fusion was not induced in cells expressing LUJV-GP, even by treatment with the buffer at pH 4 (Fig. 7B). The luciferase activities in the VSV-G-expressing cells exhibited moderate enhancement, even though syncytium formation was clearly observed. This may be due to cytotoxicity of the VSV-G in the expressing cells. Similarly, pH 3 treatment of the cells induced cytotoxicity, and thus, the expression of luciferase may have been affected.

In general, low-pH exposure is known to change the conformation of some viral GP in the absence of cellular receptors and then to abolish viral infectivity. To examine the effect of low-pH exposure on AREpv infection, the viruses were treated with the indicated pH buffer or for the indicated exposure times before infection. Infectivities of all of the AREpv, including LUJpv, were abolished after low-pH treatment and within 2 min of exposure (Fig. 7C and D). Notably, LASpv was relatively resistant to low-pH exposure in comparison to other AREpv, suggesting that conformational change of LASV-GP may be induced under more acidic pH conditions or by longer-duration exposure.

Involvement of cholesterol and sphingolipids in AREpv infection. Recently, it has been reported that Ebola virus infection requires cholesterol transporter protein, Niemann-Pick C1 (NPC1), and acid sphingomyelinase, which is the hydrolase enzyme involved in sphingolipid metabolism (31–33). In the present study, LUJV-GP-expressing cells did not exhibit cell fusion upon treatment at low pH, indicating the necessity for additional cellular factors for LUJV infection. To further examine the entry pathway and roles of lipid metabolism in AREpv infection (especially LUJpv infection), we examined the effect of chlorpromazine treatment of the cells. This chemical is widely known, not only as an inhibitor of clathrin-mediated endocytosis, but also as an inducer of lipidosis (34, 35). Even though infections by all of the AREpv were inhibited by chlorpromazine treatment in a dose-dependent manner, LUJpv and LASpv infections were drastically reduced in comparison with the other AREpv (Fig. 8A). The effects of other lipidosis-inducing drugs, imipramine, desipramine, and amitriptyline, which are known as antidepressant drugs and which cause lipid accumulation *in vitro* (33), were also examined. LUJpv and EBOpv were drastically inhibited by all of these drugs (Fig. 8B). Furthermore, a cholesterol transport inhibitor, U18666A, which is known to inhibit the function of NPC1 (36, 37), was utilized. Treatment with the chemical resulted in a dose-dependent decrease in LUJpv and EBOpv infectivities (Fig. 8C). Interestingly, these inhibitors also partially decreased LASpv infectivity, suggesting that the entry mechanisms of LASpv are similar, in part, to those of LUJpv (Fig. 8B and C). To further examine the involvement of NPC1, NPC1-deficient CHO mutant cells, CHO/A101 cells, were utilized. The infectivities of LUJpv and EBOpv were